# UNIVERSITÁ DEGLI STUDI DI PARMA

## DOTTORATO DI RICERCA IN
## "SCIENZE CLINICHE VETERINARIE"
## XXIX° CICLO

# *High-Frequency Ultrasonographic Imaging of Superficial Soft-tissue Lesions in Dogs*


Coordinatore:

Chiar.mo Prof. *Attilio Corradi*

Tutor:

Chiar.ma Prof. *Antonella Volta*

Dottoranda: *Martina Fabbi*


ANNI ACCADEMICI 2014-2016

# TABLE OF CONTENTS

**ABBREVIATIONS** ……... 5

**ABSTRACT** …..……... 6

**INTRODUCTION** ……... 7

**PART I**

• GENERAL ASPECTS

Skin ultrasound in human medicine ……..... 9

Instrumentation, examination protocol and indications ……..…..... 10

• THE REQUISITES

Canine skin: normal anatomy ……. 12

Canine skin: ultrasonographic anatomy ……. 15

Human skin: ultrasonographic anatomy ..…….. 17

# PART II

## CLINICAL APPLICATIONS and TUMOR PATHOLOGY in HUMANS AND DOGS

### • *NEOPLASTIC LESIONS*

*MALIGNANT*


- Mast cell tumor ……. 19
- Melanoma ……. 21
- Hemangiopericytoma …… 22
- Metastasis …….. 23
- Fibrosarcoma ……. 26
- Sweat gland adenocarcinoma …… 26


*BENIGN*


- Lipoma …… 27
- Hemangioma …….. 28
- Cutaneous Histiocytoma ..…….. 28
- Hepatoid gland adenoma …… 29
- Follicular tumors ……. 29
- Nodular dermatofibrosis ……. 31


*TUMOR-LIKE LESIONS*


- Infundibular cyst (epidermoid cyst) …… 32

• ***INFLAMMATORY-INFECTIOUS LESIONS***

- Cellulitis ……. 36
- Abscess ..……. 37
- Pyoderma ..…….. 39
- Granuloma …….. 40

**PART III**

AIM OF THE STUDY …….. 43

MATERIALS AND METHODS ……. 43

RESULTS ……... 47

DISCUSSION ……... 69

**CONCLUSIONS** ……. 77

**REFERENCES** ……. 79

**ACKNOWLEDGEMENTS** ……... 93

# ABBREVIATIONS (in alphabetical order)

| | |
|---|---|
| CDUS | Color-Doppler Ultrasound |
| CH | Cutaneous histiocytoma |
| HFUS | High-frequency ultrasonography |
| HPC | Hemangiopericytoma |
| IC | Infundibular cyst |
| IKA | Infundibular keratinizing acanthoma |
| MCT | Mast cell tumor |
| MET | Metastasis |
| ND | Nodular dermatofibrosis |
| US | Ultrasonography |

# ABSTRACT

A retrospective survey was perfomed on all the superficial soft-tissue nodules/masses investigated with high-frequency ultrasound between 2010 and 2015 in dogs presented to the Veterinary Teaching Hospital of University of Parma, Italy.

The aim of the study was to identify and describe the ultrasonographic features of superficial soft-tissue lesions in dogs. Moreover, the potential diagnostic value of ultrasound in differentiating benign from malignant lesions has been evaluated.

Inclusion criteria were: the use of a high-frequency probe (10-18 MHz), ultrasonographic evaluation of size, shape, borders, echogenicity, echotexture, vascularization of the lesions, and histological or cytological confirmation of lesion type.

Lesions were divided in 2 groups: benign (n.54) and malignant (n.53).

Data were evaluated with descriptive analysis and the results were compared with statistical analysis in order to identify any significant pattern to characterize the lesions.

The items collected were then discussed and compared with the literature.

# INTRODUCTION

In human medicine, the diagnosis and management of most skin diseases, both focal and diffuse, has traditionally relied on clinical and histological characteristics (Cammarota *et al*, 1998).

The recent introduction of technologically advanced ultrasound equipment using 20 MHz probes permitted the specific application of US to dermatology. The use of frequency of ≥ 20 MHz allows precise differentiation among the cutaneous layers and the recognition of tiny normal structures (eg, cutaneous adnexa) ((Mandava *et al*, 2013).

Currently, HFUS is increasingly being used in the non-invasive evaluation of various cutaneous diseases and nodules in human medicine (Mandava *et al*, 2013).

HFUS assists in the management of both inflammatory and neoplastic processes (Chiou *et al*, 2007).

It enables to perform early diagnosis, determine the degree and activity and severity of the disease and provide precise anatomical information which enables to adequately plan the surgical procedures (Diaz *et al*, 2014).

In veterinary literature, diagnosis of dermatological diseases is currently based mainly on the patient's medical history, a thorough physical examination and the use of ancillary diagnostic tests. These include microscopic examination of hair or skin scrapings, bacteriologic and fungal culture, cytologic and biopsy evaluation of skin specimens and allergy testing (Houston *et al*, 2000; Scott *et al*, 2001).

Recently, HFUS has been reported to be a reliable non-invasive technique for the evaluation of normal skin thickness in dogs and for the assessment of skin hydration in healthy dogs and in dogs with skin edema (Diana *et al*, 2004; Diana *et al*, 2008).

However, to date, the application of diagnostic US for examination of the skin has been largely limited in domestic animals. With the exception of inflammatory conditions (foreign body granulomas, abscesses), only few studies exist describing the ultrasonographic features of superficial soft-tissue lesions in dogs (Gonzalez *et al*, 1998; Armbrust *et al*, 2003; Ohlerth and Kaser-Hotz, 2003; Gnudi *et al*, 2005; Nyman *et al*, 2006; Volta *et al*, 2006; Loh *et al*, 2009).

It is however becoming apparent that sonographic characteristics of superficial soft-tissue lesions may have a role in predicting lesion type (Volta *et al*, 2006; Loh *et al*, 2009).

The aims of this study were to describe the ultrasonographic features of skin and subcutaneous lesions in dogs and to evaluate the usefulness of high-resolution grayscale and Color Doppler ultrasound to distinguish benign from malignant soft-tissue masses on the basis of ultrasonographic patterns.

The final objective is to propose HFUS in the diagnostic protocol for patients with skin lesions.

# PART I

## • GENERAL ASPECTS

### SKIN ULTRASOUND IN HUMAN MEDICINE

US has been used in the field of human dermatology for nearly 30 years (Kleinerman *et al*, 2012).

In 1979, Alexander and Miller first introduced US as a noninvasive technique to measure normal skin thickness, and in the 1980s and 1990s, HFUS was used for non invasive assessment of skin nodules and cutaneous disease (Alexander and Miller, 1979; Miyauchi *et al*, 1983; Stiller *et al*, 1994).

Studies show that HFUS is superior to clinical examination alone by providing valuable information in the detection and accurate measurement of many clinical and subclinical cutaneous lesions (Chami *et al*, 2011).

Furthermore, US is the only imaging modality useful in the evaluation of superficial cutaneous lesions that are too small to be evaluated on computed tomography (CT) or magnetic resonance imaging (MRI) (Mandava *et al*, 2013).

## INSTRUMENTATION AND EXAMINATION PROTOCOL

The evaluation of cutaneous lesions in radiology department is generally performed with linear array high-frequency transducers (operating bandwidth of 6-18 MHz) (Mandava *et al*, 2013).

A copious amount of gel is used over the surface and any hair present is displaced with gel towards the lesion margins to minimize artifacs (Mandava *et al*, 2013).

Compression is avoided in superficial lesions because this may result in false thinning or superficial nodules might move outside the field of view (Cammarota *et al*, 1998). Furthermore, small vessels and low-velocity signals could not be detected if an excessive pressure is applied (Chiou *et al*, 2007).

Grayscale and CDUS are applied to the lesion in at least two perpendicular scanning planes (Chiou *et al*, 2007).

The HFUS examination of each lesion consists of:

a) morphologic study of the structural sonographic pattern and margins;
b) measurement of the largest transverse diameter and thickness;
c) CDUS for intralesional and perilesional vessels;
d) in cases suspicious for malignancy, the surrounding areas are scanned for locoregional metastasis (Mandava *et al*, 2013).

## INDICATIONS

US has been used in the evaluation of benign and malignant neoplasms, inflammatory diseases, infectious diseases, and in the forum of cosmetic dermatology.

The current indications for HFUS in dermatology are as follows: (Cammarota *et al*, 1998; Szymanska *et al*, 2000; Schmid-Wendtner and Burgdorf, 2005; Radu *et al*, 2010; Wortsman and Wortsman, 2010; Kleinerman *et al*, 2012; ; Mandava *et al*, 2012; Mandava *et al*, 2013)

1. Measurement of thickness, invasion depth, and assessment of the borders of skin tumors, and follow-up after surgery, cryotherapy, and laser treatment (e.g. malignant melanoma, basal cell carcinoma, hemangioma, fibroma, seborrheic wart);
2. Monitoring the course and therapeutic efficacy of the treatment of diseases with skin sclerosis (e.g. morphea, systemic scleroderma, scleroderma-like diseases), edematous (e.g. lipodermatosclerosis) and chronic inflammatory dermatoses (e.g. psoriasis);
3. Monitoring the effects of topical and systemic drugs on the skin (e.g. corticosteroids, estradiol);
4. Evaluation of allergic dermatitis, nodular erythema, dermatomyositis, sarcoidosis, lymphedema of the limbs, wound healing, scars and follow-up of localized burn lesions;
5. Evaluation of exogenous components like foreign bodies and cosmetic fillers in the skin;
6. Evaluation of nail involvement in systemic diseases and nail bed lesions like glomus tumors, nail bed cysts, subungual exostosis.

# • THE REQUISITES

## CANINE SKIN: NORMAL ANATOMY

The skin is the largest single organ in the canine body (Paterson, 1998). It provides protection from physical, chemical, and microbiological injury and, at the same time, preserves the internal environment of all other organs by functioning as an effective barrier against the loss of water, electrolytes, and, macromolecules (Scott *et al*, 2001).

The skin is responsible for temperature regulation and for perception of heat, cold, pressure, pain and itch, through nerve sensors (Paterson, 1998). Finally, the skin surface has both antibacterial and antifungal properties and these, in combination with its immunoregulation function, help prevent the development of infection and neoplasia.

The skin is composed of 3 distinct layers: an outer thin epithelium, the ***epidermis***, an underlying thicker layer of connective tissue, the ***dermis***, and the thickest and innermost layer, the ***subcutis*** (Fig. 1).

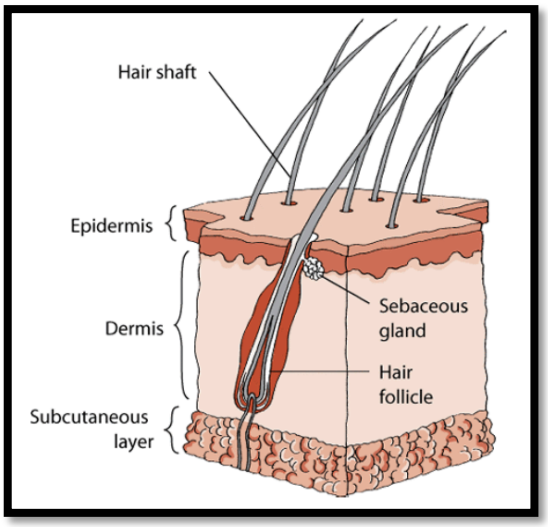


Fig. 1. The anatomy of a dog's skin includes 3 major layers, as well as hair follicles and sebaceous glands (Figure adapted from Kahn and Line, 2007).

***Epidermis***

The epidermis provides protection from foreign substances and is the most metabolically active layer of the skin. The epidermal layer is a stratified, continuously renewing set of primarily keratinocytes (85%) that progressively differentiate from the dermis in a superficial direction.

Other cells included in the epidermal layer are melanocytes, Langerhans cells, and Merkel cells (Paterson, 1998).

***Dermis***

The dermis is the middle layer of the skin and its thickness varies depending on the hair cover and epidermal thickness of the region of the body. This layer is primarily responsible for tensile strength and elasticity. The dermis supports and nourishes the epidermis and skin appendages, through blood vessels carrying nutrients.

Other functions of the dermis include regulation of cell growth and proliferation, adhesion, migration and differentiation of cells, and wound healing (Scott *et al*, 2001).

***Subcutis (Hypodermis)***

The subcutis is the innermost and the thickest layer of the skin. This layer contains a network of fibrous bands that are connected to the dermis and the underlying fascial sheets. These fibres divide the adipocytes into many lobules.

The subcutaneous fat provides insulation; a reservoir for fluids, electrolytes, and energy; and acts a shock absorber (Abramo *et al*, 2009).

***Skin appendages (adnexa)***

Hair follicles, sebaceous and sweat glands, and claws, are skin appendages that grow out of the epidermis and dermis.

The reported mean thickness of the skin of dogs ranges from 0.5 to 5 mm (Scott *et al*, 2001). In general, skin decreases in thickness from dorsal to ventral on the trunk and from proximal to distal on the limbs. Skin is thinnest on the ears, axillary, inguinal, and perianal areas, while is thickest on the forehead, dorsal neck, thorax, rump, and base of the tail (Scott *et al*, 2001).

Thickness of the skin varies widely in dogs due to the great polymorphism, which characterizes the various canine breeds (Scott *et al*, 2001). The greatest skin thickness in one study was detected for a Sharpei, given the abundant mucinous dermal intercellular material characteristic of this breed. In the same study, the lowest skin thickness measurements were found in a Zwergpinscher and a Toy Poodle (Diana *et al*, 2004).

Furthermore, hydration status was found to be correlated with skin thickness in dogs (Diana *et al*, 2008).

In humans, thickness of the skin varies among parts of the body and may be influenced by several factors including age, sex, and distribution of body fluid (De Rigal *et al*, 1989; Gniadecka *et al*, 1994(a); Gniadecka *et al*, 1994(b); Seidenari *et al*, 1994). These factors influence the tension and elasticity of the skin and could be considered also valid for the dog (Young *et al*, 2002; Diana *et al*, 2004).

In human, aging of the skin is accompanied by a decreased in skin thickness as a result of reduction of water, protein and collagen content (Gniadecka *et al*, 1994(b)). Furthermore, the skin of the females is thinner than that of the male because female sex hormones influence water retention (Seidenari *et al*, 1994).

# CANINE SKIN: ULTRASONOGRAPHIC ANATOMY

Comparison between histological and ultrasonographic appearance of the skin revealed that layering of canine skin (epidermis and dermis) and the subcutaneous tissue may be recognized and measured by use of HFUS (Diana *et al*, 2004).

B-scans provide images that resemble reliably anatomic cross sections of scanned tissues.

Normal skin is 2 to 3 mm thick with a laminar hyperechoic appearance (Zwingenberger *et al*, 2015).

The ultrasonographic pattern of canine skin is characterized by 3 distinct, defined echogenic layers corresponding to the epidermal entry echo, epidermis and dermis, and subcutaneous tissues (hypodermis) (Fig. 2 and 3).

**a.** The first hyperechoic layer (line) is created as a result of the differing acoustic impedance between the coupling gel and stratum corneum of the skin surface. This line corresponds to the epidermal entry echo described by human dermatologists, and its echogenicity depends on the thickness of the stratum corneum and the amount of air trapped between the keratotic scales (Poziniak *et al*, 1989)

**b.** The second layer corresponds to the epidermis and dermis; it is less echogenic and considerably thicker than the epidermal entry echo. Two different patterns have been described for this layer in dogs and are probably related to the differing amounts of dermal fluid storage, which influences its echogenicity (Diana *et al*, 2004).

The first pattern includes a homogeneous layer (Fig. 2), while the second includes two distinct bands with clearly differing echogenicity (Fig. 3). The inner band is more hypoechoic due to a more abundant interstitial water content.

**c.** The third and thickest layer, characterized by an inhomogeneous hypoechoic pattern with thin linear hyperechoic bands, corresponded to the subcutaneous tissues. Its ultrasonographic appearance is related to the primarily adipose nature of the subcutis which contains connective septa (Fig. 2 and 3) (Fornage *et al*, 1993; Milner *et al*, 1997; Szymanska *et al*, 2000).

The clearly recognizable and defined dermis-subcutis interface is probably related to the large difference in acoustic impedance between the dermis and subcutaneous layer (Fornage *et al*, 1993).

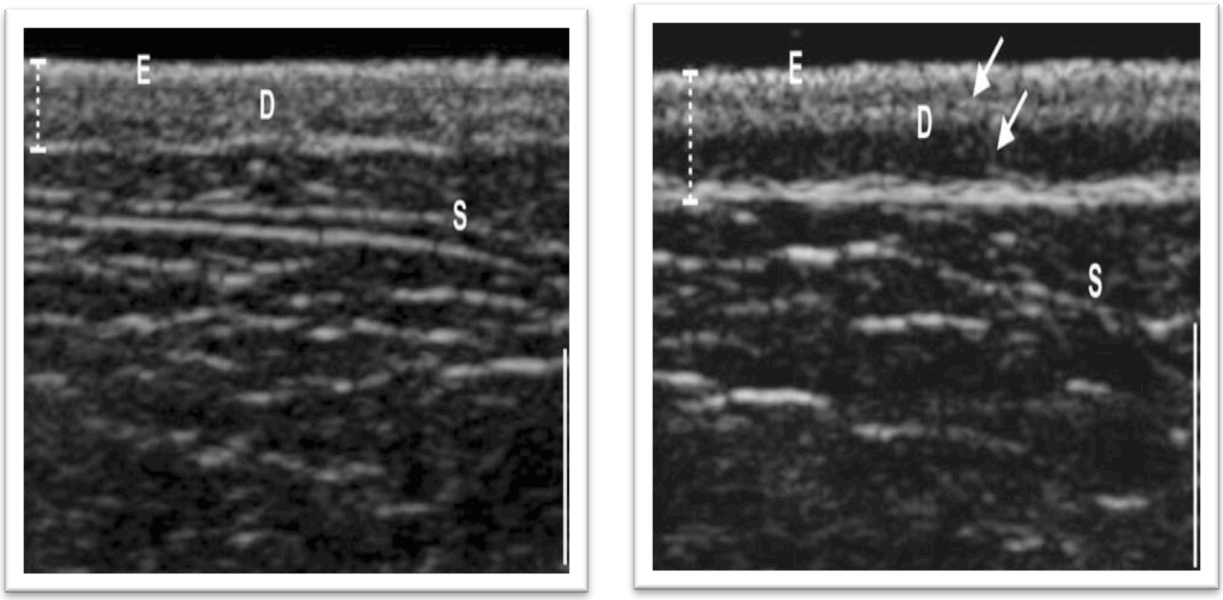


Fig. 2. and 3. Representative ultrasonogram of normal canine skin obtained by use of a 13-MHz linear-array transducer. Three distinct layers are clearly recognizable: epidermal entry echo (E), the epidermis plus dermis (D), and the subcutaneous tissues (S). In Fig. 3 (on the right), the echogenicity of the second layer (epidermis plus dermis; D) is not uniform, and two distinct bands with differing echogenicity are recognizable (arrows). A measurement of skin thickness was obtained (dotted line). Bar = 5 mm. (Figure adapted from Diana *et al*, 2004).

Skin adnexa were not identified in the study of Diana *et al* (2004), where a frequency probe of 13 MHz was used.

However, recognition of skin adnexa (hair follicles, shafts and sebaceous glands) is considered theoretically possible in dogs as in humans, with a frequency of at least 20 MHz (Fornage *et al*, 1993).

# HUMAN SKIN: ULTRASONOGRAPHIC ANATOMY

The ultrasonographic features of the skin show similarities between humans and dogs.

In the ultrasound image of the healthy skin in man, as in the dog, three basic layers may be distinguished: epidermal echo, dermis and subcutaneous tissue (Altmeyer *et al*, 1992; Nowicki, 2004), which correspond to the anatomical structure of the skin (Martini, 2007).

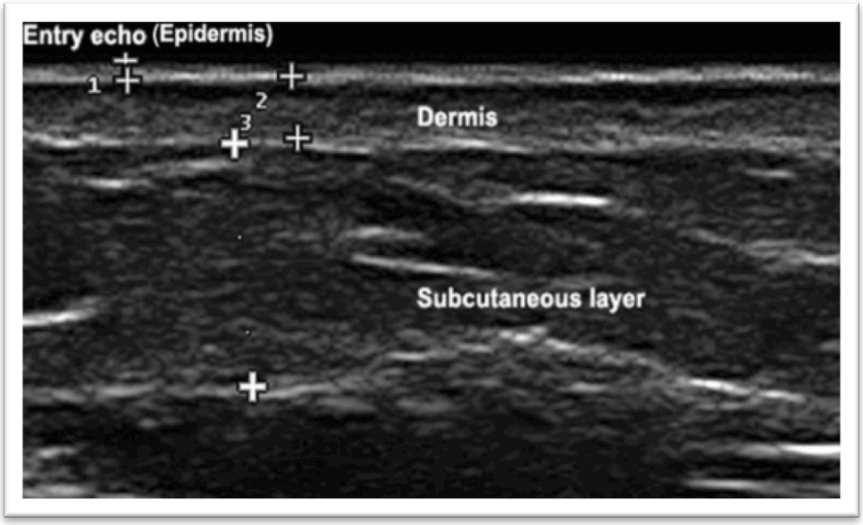


Fig. 4. HFUS of human skin at 18 MHz shows the three distinctive layers of epidermal "entry echo,"(1) dermis (2,3), and subcutaneous tissue (Figure adapted from Mandava *et al*, 2012).

A well-defined hyperechoic band known as epidermal "entry echo" is present at the interface between the transducer and the skin (Fig. 4).

Underneath, two distinct bands with differing echogenicity can be easily recognized in the dermal layer, corresponding to the papillary and the reticular dermis (Fig. 4 and 5) (Martini, 2007). The upper layer is usually thinner and presents decreased echogenicity in comparison to the lower one. This diversification of the dermal image results from the anatomical structure of the skin. The papillary dermis includes a lower number of the collagen fibres and they are much thinner.

Therefore, they reflect ultrasounds in a weaker way. This results in lower echogenicity as compared to the echoes of the collagen fibres situated in the lower layer – they are thicker and thus, produce stronger echoes (Mlosek *et al*, 2013).

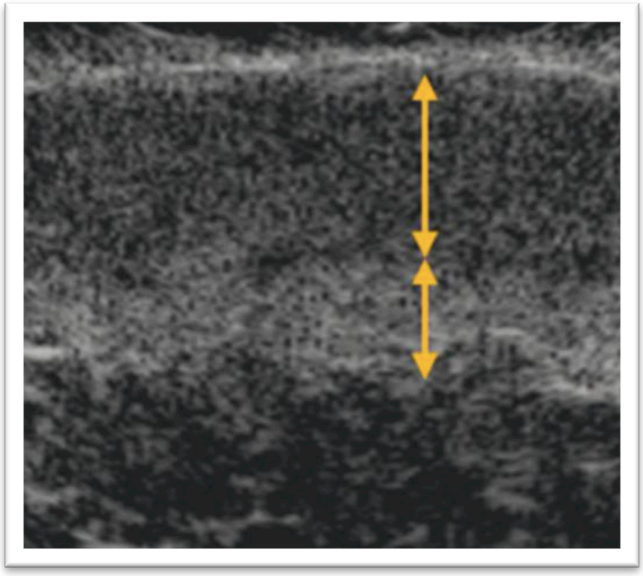

Fig. 5. High-frequency ultrasound image (48 MHz) of the dermis with its visible division into the upper hypoechoic and lower hyperechoic layers (Figure adapted from Mlosek *et al*, 2013).

On the other hand, a clearly defined demarcation between the papillary and reticular dermis is not evident in the skin of domestic carnivores on histology (Scott *et al*, 2001). The two distinct bands visualized on HFUS in the dermal layer of some dogs are probably related to different amount of dermal fluid storage (Fig. 3) (Diana *et al*, 2004).

The third layer, subcutaneous tissue, is hypoechoic with hyperechoic connective tissue septa separating the adipose lobules (Fig. 4) (Fornage *et al*, 1993; Milner *et al*, 1997).

# PART II

# CLINICAL APPLICATIONS and TUMOR PATHOLOGY in HUMANS AND DOGS

## • *NEOPLASTIC LESIONS*

*MALIGNANT*

### *Mast cell tumor (MCT)*

Cutaneous MCTs account for 7% to 21% of all canine skin tumours, and are considered the most common canine skin tumours submitted for histology and diagnosed in veterinary teaching hospital populations (Welle *et al*, 2008).

The aetiology of MCT is unknown, but the well-documented breed predispositions (Boxer, Boston Terrier) likely indicate an underlying genetic component (Marconato *et al*, 2012(a)).

Cutaneous MCTs are most common on the trunk (50–60%), followed by the extremities (25–40%), and the head and neck (10%) (Welle *et al*, 2008). The scrotum, perineum, back and tail are less commonly affected (Goldschmidt and Shofer, 1992).

The biological behaviour of cutaneous MCTs is extremely variable, ranging from benign solitary nodule to metastastic disease (Marconato *et al*, 2012(a)).

Definitive diagnosis of cutaneous MCTs requires cytological/histological examination (Welle *et al*, 2008). Ultrasound is currently used in the clinical staging of mast cell disease, but not as a primary approach to skin lesions (Welle *et al*, 2008).

However, ultrasonographic features of cutaneous MCTs have been described (Loh *et al*, 2009). The

combination of a homogeneous echotexture, a well-defined margin and the presence of a subcapsular vessel was considered highly predictive of MCTs in that study (Loh *et al*, 2009).

Mast cell tumor, also known as "Mastocytoma", has been described also in humane literature, with young children being overrepresented (Wortsman and Bouer, 2013). Spontaneous involution is common, and they are usually not associated with systemic involvement.

Mastocytomas appear clinically as a solitary reddish-brown, pink nodule or plaque most frequently on the extremities, torso or head (Wortsman and Bouer, 2013).

On sonography, solitary mastocytomas presents as hypoechoic band-like, oval or fusiform shaped dermal lesions that usually follow the axis of skin layers. On CDUS, there is a variable pattern of blood flow going from hypovascular to hypervascular lesions (Wortsman and Bouer, 2013).

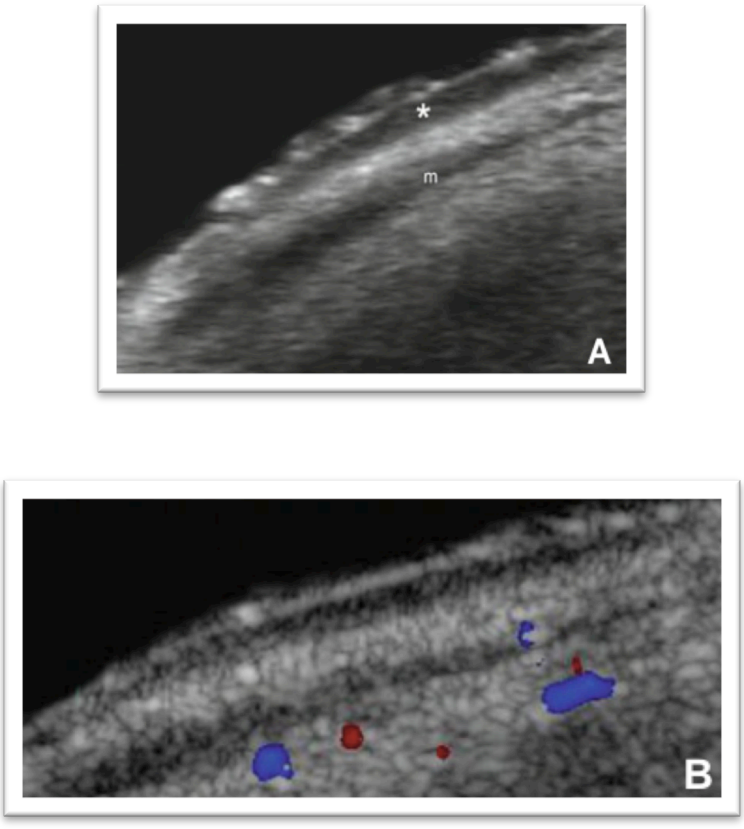


Fig. 6. (A,B) Grey scale and CDUS images of a solitary mastocytoma in the left lower eyelid in a child. A) A hypoechoic dermal plaque (white asterisk) which follows the axis of the skin layers is seen. B) Lack of vascularity is seen in the lesional area. m, orbicularis muscle (Figure adapted from Wortsman and Bouer, 2013).

## *Malignant melanoma*

Melanomas are neoplasms originating from melanocytes and have been described in both human and most animal species (Nishyia *et al*, 2016).

In dogs, melanomas most commonly occur on the skin, in the mouth, and on the digits or in association with the nail bed (Marconato *et al*, 2012(b)).

Unlike in humans, the majority of skin melanomas are benign in dogs, however oral and digit/nail bed melanomas tend to be malignant, with the potential to locally invade tissues and underlying bone, as well as spread to other parts of the body (regional lymph nodes and lungs) (Marconato *et al,* 2012(b)).

In human medicine, melanoma is considered a highly malignant but curable skin cancer and early detection is the basis for reducing the mortality rate (Mandava *et al*, 2013).

HFUS is currently used in the loco-regional staging of cutaneous melanoma in people (Catalano *et al*, 2010).

Ultrasonographic features of melanoma include solid, homogenously hypoechoic lesion with a thin "entry echo" and quite well-delimited contours (Fig. 7) (Mandava *et al*, 2013).

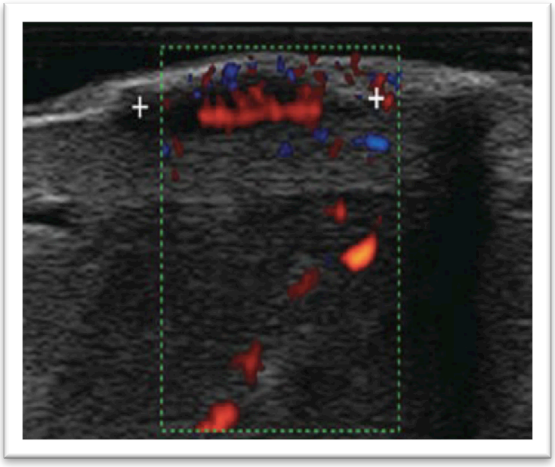

Fig. 7. HFUS of a cutaneous melanoma in a man shows a well-defined, solid, homogenously hypoechoic lesion in the dermis with multiple vessels arising from the base, suggestive of high vascular density (Figure adapted from Mandava *et al*, 2013).

The histopathologically measured thickness of melanoma (Breslow index) is the single most important prognostic factor in human beings and can be measured accurately and noninvasively by using HFUS (Breslow, 1970; Szymanska *et al*, 2000).

The tumor thickness and the vascular density identified by Color Doppler are significantly correlated with metastatic potential and dissemination in melanomas (Lassau *et al*, 2006).

Furthermore, HFUS is currently used in the detection of skin and subcutaneous metastases of melanoma, being this procedure considered more sensitive and specific than palpation (Catalano *et al*, 2010).

## *Hemangiopericytoma (HPC)*

HPC is a malignant mesenchymal neoplasm deriving from vascular pericytic contractile cells around vessels and has been described in both human and dogs (Namazi *et al*, 2014).

Skin and subcutaneous tissues of limbs are overrepresented site of development in dogs (Marconato *et al*, 2012(c)). In this species, HPCs tend to have the lowest metastatic rate of all the soft tissue sarcomas (<5%), although local regrowth of the tumor is common after conservative surgical removal (Marconato *et al*, 2012(c)).

In human, HPC commonly involves the lower extremities, pelvis, and retroperitoneum (Kransdorf and Murphey, 2000).

The typical presentation on US is heterogeneous hypoechogenicity, well-defined or infiltrated margins, scalloped contour, solid and/or necrotic content, moderate to large size and marked hypervascularity on CDUS. HPCs may exhibit prominent serpentine vessels—a finding that reflects rich tumor vascularization (Chiou *et al*, 2007).

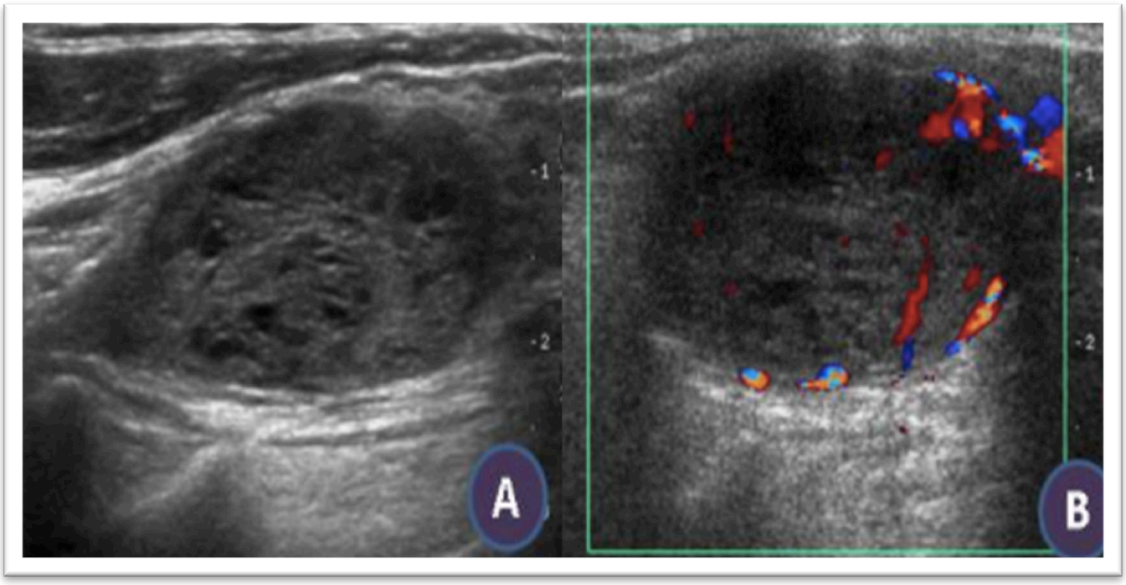


Fig. 8. (A,B) B mode and CDUS of a soft tissue nodule, confirmed to be a hemangioperycitoma, in left supraclavicular region in a man. Hypoechoic relatively well-defined edges nodule, moderately hypervascular with tiny cistic lesion inside (Figure adapted from Hervas *et al*, 2013).

In dogs, ultrasonographic aspects of soft tissue sarcomas have been mentioned in a paper, but no specific reference to HPC was provided in that article (Loh *et al*, 2009).

## *Metastasis (MET)*

Superficial soft-tissue METs are rarely reported in both human and veterinary literature (Reed *et al*, 2012; Tunio *et al*, 2013; Vignoli *et al*, 2013).

Skin, subcutaneous and muscular METs are usually encountered in end-stage neoplasms; consequently, the appearance of skin nodules is generally considered a terminal manifestation of a neoplastic disease (Giovagnorio *et al*, 2003). Ultrasonographic features of superficial soft-tissue METs have been described in human beings and include hypoechoic nodules, with smooth or lobulated contours and with detectable internal Color and Doppler signal (Surov *et al*, 2014).

A polycyclic shape, that is irregular shape with multiple tissue protrusions along the borders (Fig. 9), has been described as the the most indicative sign of skin metastasis in a human study (Giovagnorio *et al*, 2003).

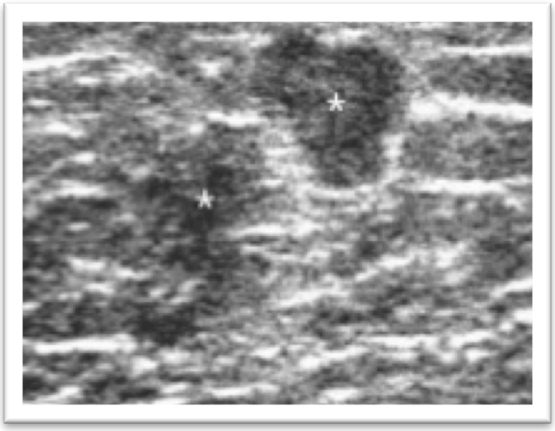

Fig. 9. Two moderately hypoechoic, rather homogeneous 1.1- and 1.2-cm-wide nodules (asterisks) localized in the subcutaneous fat of the lateral thoracic wall in an asymptomatic 47-year-old man. Histologic examination and follow-up revealed metastasis from a previously undiagnosed melanoma of the foot (Figure adapted from Giovagnorio *et al*, 2013).

Ultrasonographic features of superficial soft-tissue METs are lacking in the veterinary literature. To date, only one report describing ultrasonographic characteristics of skeletal muscle metastases in a dog with hemangiosarcoma has been reported (Fabbi *et al*, 2016).

In that case, well-defined, avascular, hypoechoic solid nodules, with irregular shape and margins, were identified within the skeletal musculature of the thoracic wall (Fig. 10 A and B). Irregular margins on ultrasound corresponded to infiltration of the tumor of the surrounding tissue on histologic examination (Fig. 11).

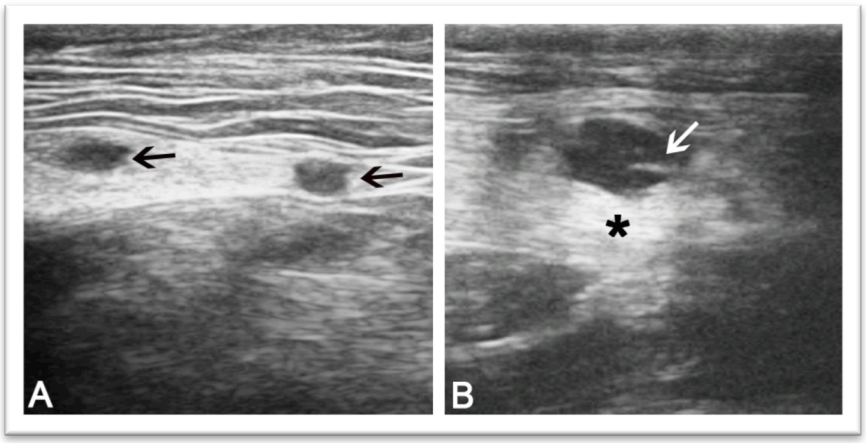


Fig. 10. (A,B). B-mode ultrasonographic image of the left thoracic wall, transverse view. (A) Two solid, well-defined hypoechoic nodules, with a relatively homogenous echotexture within the skeletal muscle layer of the chest wall. Both nodules show a thin, linear, hyperechoic structure at the caudal pole (arrows). (B) Detail of a third hypoechoic nodule, showing irregularly shaped and ill-defined margins. Mild posterior acoustic enhancement is present (arrowheads). (figure adapted from Fabbi *et al*, 2016).

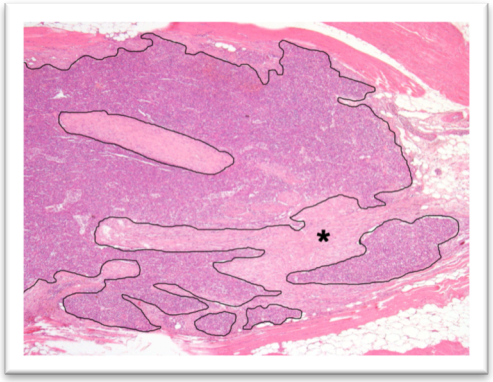

Fig. 11. Histologic section of one skeletal metastasis of the hemangiosarcoma showing the neoplastic proliferation (highlighted area) and the fibrous band (asterisk) visualized on US. 100× H&E stain objective. (Figure adapted from Fabbi *et al*, 2016).

## *Fibrosarcoma*

Fibrosarcoma is a malignant mesenchymal neoplasm characterized by the presence of immature proliferating fibroblasts (Marconato *et al*, 2012(c)). The most common form of fibrosarcoma in dogs is a solitary mass, typically found on the head, limbs, or oral cavity (Liptak and Forrest, 2007).

In dogs, fibrosarcoma represents the 15% of all subcutaneous tumors (Marconato *et al*, 2012(c)).

Fibrosarcomas present a rapid infiltrative growth, they recur after surgical excision, but metastases are not very common; they are estimated at about 25% (Marconato *et al*, 2012(c)).

In human, ultrasonographic aspects of fibrosarcoma typically reveal heterogeneous hypoechogenicity, ill-defined margins, ovoid contour, solid content, large size, mild vascularity on CDUS (Chiou *et al*, 2007).

Ultrasonographic features of soft tissue sarcomas in dogs have been described in two studies, but no precise referral to fibrosarcoma was given (Nyman *et al*, 2006; Loh *et al*, 2009). Furthermore, no ultrasonographic features specific for sarcoma were found in those papers.

## *Sweat gland adenocarcinoma*

Apocrine sweat gland adenocarcinomas are relatively uncommon skin tumors in dogs, but when they occur, they tend to be malignant (90%) (Simko *et al*, 2003; Marconato *et al*, 2012(b)).

This tumor most commonly occurs where the legs meet the trunk and near the groin. Treeing Walker Coonhounds, Norwegian Elkhounds, German Shepherds, and mixed-breed dogs are most at risk (Marconato *et al*, 2012(b)).

Biological behaviour is locally aggressive, with low metastatic rate (Marconato *et al*, 2012(b)).

## *BENIGN*

### *Lipoma*

Lipomas are benign mesenchymal tumors comprised of mature adipocytes and have been described in both human and veterinary literature (Weiss, 1996; Volta *et al*, 2006). They are typically soft, freely movable masses of varying sizes within the subcutis, but intramuscular location is also reported (Thomson *et al*, 1999; Inampudi *et al,* 2004; McTighe and Chernev, 2014).

Typical ultrasonographic features of lipomas include oval, well-defined, encapsulated, striated mass (Fig. 12) (Volta *et al*, 2006; Chiou *et al*, 2009). The presence of striations is interpreted as ingrowth of connective tissue from the capsule becoming the fibrous stroma (Volta *et al*, 2006; Chiou *et al*, 2007).

Although lipomas usually have a relatively hyperechoic echotexture, they have been reported to have isoechoic, hyperechoic, or hypoechoic appearances (Fornage and Tassin, 1991; Volta *et al*, 2006).

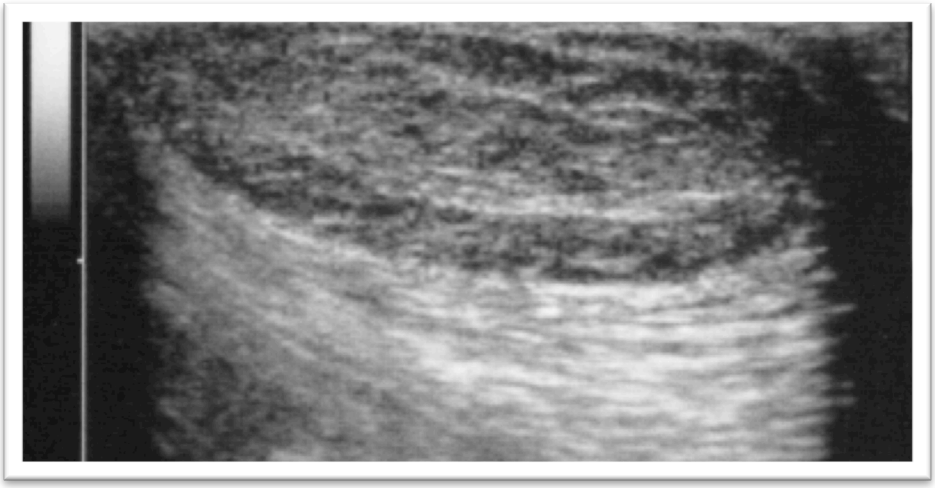

Fig. 12. Striped appearance, sharpe edges and a thin hyperechoic capsule in an oval lipoma in the elbow region in a dog (Figure adapted from Volta *et al*, 2006).

## *Hemangioma*

In dogs, cutaneous hemangiomas are benign growths, which originate from endothelial cells located in the skin and/or subcutaneous tissues (Cooley *et al*, 1997).

In human, hemangioma is the most frequently encountered vascular soft tissue abnormality, comprising approximately 7% of all benign soft tissue tumors (Chiou *et al*, 2007). Infants are overrepresented (Dubois *et al*, 1998).

The typical ultrasonographic pattern described in humane literature include lesions with heterogeneous echogenicity, ill-defined margins, solid and cystic composition, and hypervascularity (Paltiel *et al*, 2000).

Echogenic rim, good compressibility and the presence of phleboliths have also a very high positive predictive value for hemangioma (Chiou *et al*, 2007).

## *Cutaneous Histiocytoma (CH)*

Canine CHs are benign neoplasms that usually occur on the ears, face, and distal extremities of young dogs (Marconato et al, 2012(d)). The age-specific incidence rate for CH drops precipitously after 3 years, although CHs do occur in dogs of all ages (Marconato *et al*, 2012(d)).

CHs usually occur as solitary lesions that undergo spontaneous regression within 3 months (Marconato *et al*, 2012(d)).

Ultrasonographic features of 6 benign CHs have been mentioned in a paper and include homogenously isoechoic lesions with the surrounding tissue (Nyman *et al*, 2006). However, no clear information about margin and vascularization of the lesions was provided in that paper.

## *Perianal (hepatoid) gland adenoma*

Perianal adenoma is a benign tumor that originates from the sebaceous glands which surround the anus in dogs. The hairless area of the anal ring is the most common site, but tumors at the base of the tail, prepuce, thigh, and dorsal midline are also reported (Marconato *et al*, 2012(b)).

This tumor is also known as hepatoid gland tumors because, at the cellular level, perianal adenomas resemble hepatocytes.

Perianal adenomas are most common in older intact male dogs and typically act benign.
These tumors can be solitary or multiple and are dependent on the presence of testosterone. Perianal adenomas typically regress with orchiectomy of the dog (Marconato et al, 2012(b)).

## *Follicular tumors*

Follicular tumors are included in the group of well-differentiated neoplasms since they are mostly benign tumors arising from different parts of the follicle structure (Gross *et al*, 1992).

### ***Infundibular keratinizing acanthoma (IKA)***

IKA is a rare epithelial benign follicular canine neoplasm that evolves rapidly, forming a solitary or multiple firm, flask-shaped cystic nodules with keratin in their centres (Tavasoly *et al*, 2014).

Young-to middle aged, male dogs are predisposed. Most of this tumor occurr on the back, neck, head, and the shoulders.

This tumor is not locally invasive neither metastatic, but can ulcerate and rupture, releasing keratin into surrounding tissues, evoking a pyogranulomatous and granulomatous inflammatory response.

IKA has been described also in human literature. However, although many respects exist between man and dog, these tumors are not considered identical entities (Tavasoly *et al*, 2014).

***Trichoepitelioma***

Trichoepitelioma represents the 80% of all follicular tumors in dogs. It usually appears as a single nodule, different sized. Lumbar region, thorax and thigh are the most common sites (Marconato *et al*, 2012(b)).

Golden Retriever, Basset Hounds and German Sheperd are predisposed breeds.

The malignant counterpart (malignant trichoepitelioma) is considered rare.

In human, trichoepitelioma is characterized by multiple painless flesh colored or erythematous papules with a simmetrical distribution on the face (Wortsman and Bouer, 2013).

On sonography, this benign condition shows a diffuse hypoechoic plaque thickening of the dermis with multiple and tiny hyperchoic spots (Fig. 13). These tumors usually show hypovascularity on CDUS (Wortsman and Bouer, 2013).

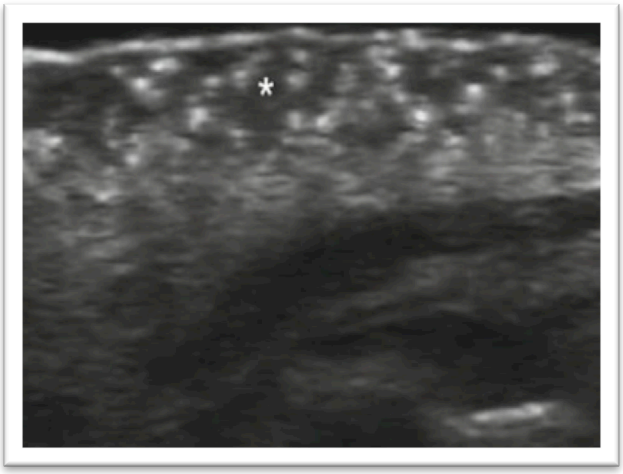


Fig. 13. Grey scale US image of a trichoepitelioma in a man (right nasofold line and upper lip, transverse view) shows a thick hypoechoic dermal plaque lesion (asterisk) with hyperechoic spots (Figure adapted from Wortsman and Bouer, 2013).

## *Nodular dermatofibrosis*

ND is a paraneoplastic syndrome described in German Sheperd dogs, and it is characterized by the development of multiple, cutaneous nodules of collagenous origin in association with renal cystadenocarcinoma or cystadenoma (Turek, 2003). The disease is inherited in an autosomal dominant pattern (Lium and Moe, 1985).

Skin lesions consist of multiple, firm, well-circumscribed nodules, ranging in diameter from 2 to 5 mm and located in the dermis or subcutis (Atlee *et al*, 1991; Moe *et al*, 1997). These lesions are localized primarily to the extremities, although distribution can be diffuse (Marconato, 2012).

Histologically, nodules consist of irregular bundles of dense, well-differentiated collagen fibres in the dermis or subcutis with no sharp demarcation from surrounding connective tissue (Gilbert *et al*, 1990; Atlee *et al*, 1991).

ND almost always anteceds systemic signs of illness related to tumour-induced renal failure or metastasis by months to years (Moe and Lium, 1997).

Although renal and skin biopsy are necessary for confirmation, the concurrent characteristic skin lesions and morphologic renal changes in a German Sheperd is considered strongly suggestive of the diagnosis (Turek *et al*, 2003).

## *TUMOR-LIKE LESIONS*

### *Infundibular cyst (IC)*

ICs are common "tumor-like" skin lesions in humans and dogs, which arise from the infundibular portion of the hair follicle and contain keratin (Lee Gross *et al*, 2005; Huang *et al*, 2011).

Because of the histopathologic similarity between infundibular and epidermal keratinisation patterns, some ICs are still classified as epidermal cysts, epidermoid cysts, or epidermal inclusion cysts in both human and veterinary literature (Lee Gross *et al*, 2005; Park *et al*, 2010).

ICs may present as solitary or multiple, firm to fluctuant, intradermal and/or subcutaneous, well-circumscribed nodules ranging from 0.2 to 2 cm in dogs and from 1 to 5 cm in humans (Cooper 1996; Lee *et al*, 2001; Raskin, 2016).

In people, ICs are most often found in the scalp, face, neck, trunk and back (Kirkham, 1997) while the dorsum and extremities are overrepresented sites in dogs (Goldschmidt and Shofer, 1992; Raskin, 2016).

Definitive diagnosis of ICs requires histological examination, both in humans and dogs (Lee *et al*, 2001; Lee Gross *et al*, 2005; Park *et al*, 2010).

In people, HFUS is currently used in the diagnosis of ICs, as it is considered superior to clinical examination alone due to the valuable information provided for the detection of these lesions (Lee *et al*, 2001).

On US, ICs are usually well-circumscribed, oval shaped, mildly echogenic and solid-appearing masses, with scattered linear echogenic reflections, increased through-transmission and no Doppler flow (Kim *et al,* 2011; Lee *et al,* 2001).

The intralesional bright echogenic foci are related to the presence of scattered keratin debris (Lee *et al,* 2001, Huang *et al,* 2011). When keratin debris is disposed as concentric laminations, a peculiar "onion-ring" appearance, comprising of alternating and concentric hyperechoic and hypoechoic ringlike shadows, results on US (Fig. 14) (Crystal and Shaco-Levy, 2005).

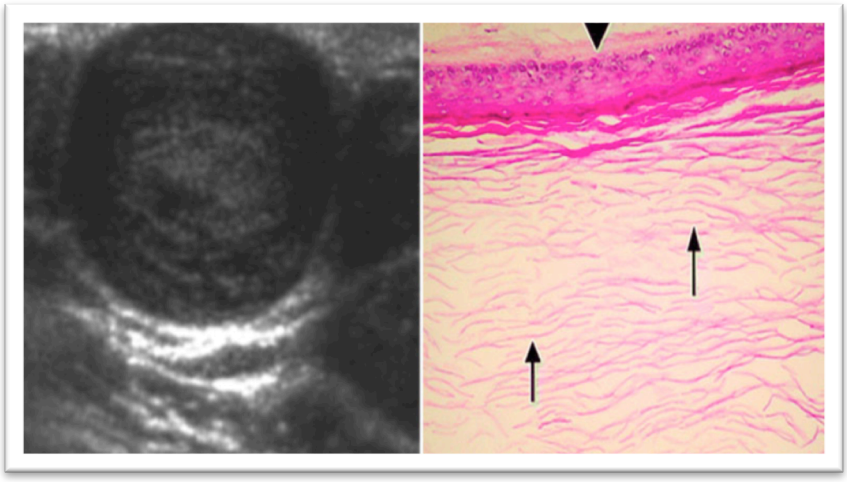

Fig. 14. Epidermal inclusion cyst of left breast in a 65-year-old woman. US shows solid, heterogeneously hypoechoic mass with alternating hypoechoic and hyperechoic concentric rings that look like onion rings On photomicrograph, lesion is lined by epidermal-type epithelium (*arrowhead*) and contains abundant lamellated keratin (*arrows*) pathognomonic for epidermal inclusion cyst (H and E ×200) (Figure adapted from Crystal and Shaco-Levy, 2005).

Ruptured ICs can result in internal vascularity (70%) secondary to the local irritant effect of leaked keratin (Yuan *et al*, 2012).

Other sonographic features such as the "pseudotestis" (Fig. 15), "target" and "tram track" (Fig.16) pattern, have been described as distinctive for ICs in humans (Lee *et al*, 2001; Rahul *et al*, 2015).

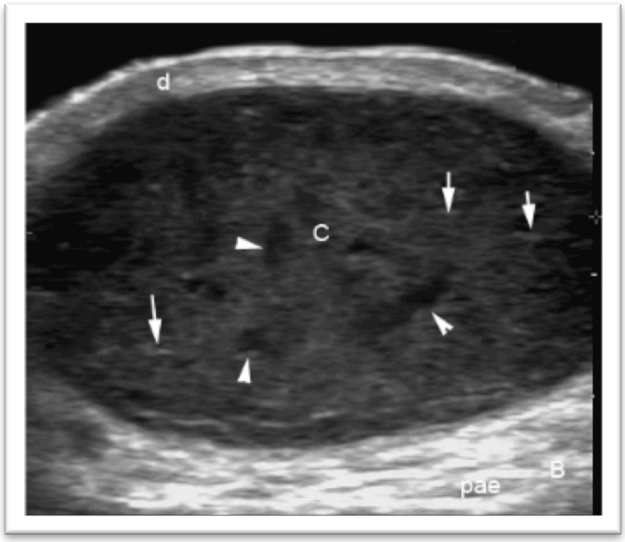


Fig. 15. Pseudotestis appearance in intact epidermal cyst. US image demonstrate filiform anechoic bands (arrowheads) and hyperechoic lines (arrows) within the cysts. Notice the posterior acoustic enhancement (pae) at the bottom of the cysts. d is dermis (Figure adapted from www.sonoskin.com).

Fig. 16. Tram-track appearance of an intact epidermal cyst. US transverse image obtained with a 15 MHz high-frequency linear probe showing a well-encapsulated heteroechoic mass. The mass also shows multiple linear parallel alternating echogenic and hypoechoic lines (arrow) (Figure adapted from Rahul *et al*, 2015).

## • *INFLAMMATORY-INFECTIOUS LESIONS*

In the field of inflammatory conditions of superficial soft-tissues, US may help to:

(1) differentiate acute or chronic infection from tumors or non-infective inflammatory conditions with a similar clinical presentation;

(2) localize the site and extent of infection (e.g. subcutaneous, muscle, bursa, tendon sheath, joint);

(3) ascertain the form of infection (e.g. cellulitis, pre-abscess, abscess);

(4) identify precipitating factors (e.g. foreign bodies, fistulation);

(5) provide guidance for diagnostic or therapeutic aspiration, drainage or biopsy (Cardinal *et al*, 2001).

The main inflammatory conditions we focus on in this thesis are:

- Cellulitis

- Abscess

- Pyoderma (folliculitis)

- Granuloma

## *Cellulitis*

Cellulitis is a severe suppurative infection occurring along subcutaneous and fascial planes and has been described in both humans and dogs (Chau and Griffith, 2005; Bigham and Nourani, 2009).

This condition usually results from a *Streptococcus pyogenes* or *Staphylococcus aureus* infection (Cardinal *et al*, 2001).

US is usually the first investigation to evaluate a clinical suspicion of cellulitis in human beings (Adhikari and Blavais, 2012).

The sonographic findings of cellulitis vary with the site and severity of infection (Chau and Griffith, 2005). In the early stages, skin and subcutaneous tissues appear hyperechoic and thickened. Later, tissues may show distorted architecture and appear marbled with fusiform or linear anechoic to hypoechoic areas (fluid) dispersed randomly in a hyperechoic background (fat and connective tissue) (Chau and Griffith, 2005; Zwingenberger *et al*, 2015). This appearance, called "cobblestone", depends on the amount of perifascial fluid, the degree of edema, and the orientation of the interlobular fat strands (Fig. 17).

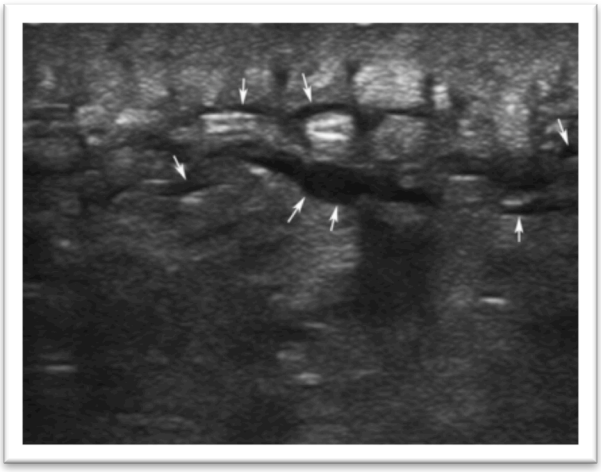

Fig. 17. The cobblestone appearance is shown as fluid (arrows) surrounding echogenic structures in the subcutaneous tissue (Figure adapted from Adhikari and Blaivas, 2012).

However, the “cobblestone” appearance is not, in itself, diagnostic of cellulitis as similar appearances occur in subcutaneous oedema, resulting from non-infective conditions such as venous insufficiency, lymphedema or cardiac failure (Chau and Griffith, 2005).

In case of cellulitis, Colour or power Doppler imaging may show concurrent hyperaemia within the subcutaneous tissues (Adhikari and Blaivas, 2012).

Finally, cellulitis may progress to preabscess or abscess formation over time.

### *Abscess*

An abscess is a localized collection of pus, often with a component of surrounding cellulitis.

The most common causative agent is *Staphylococcus aureus* (Fayad *et al*, 2007).

Ultrasonographic appearance of abscess has been described in both human and veterinary literature (Adhikari and Blaivas, 2012; Zwingerberger *et al*, 2015).

Abscesses are usually somewhat spherical with irregular or lobulated borders. The margins may be well circumscribed or poorly defined, blending with the surrounding tissues (Adhikari and Blaivas, 2012).

The gray-scale appearance of a cutaneous abscess is highly variable depending on the location, maturity, and contents of the abscess cavity.

Abscesses may or may not be organized. Nonorganized abscesses can be seen as hypo and hyperechoic collections, irregular, with a variable degree of vascularization in the periphery (Diaz, 2014).

The organized abscesses show a well-defined hypoechoic collection with peripheral pseudo-

capsule (Fig. 18); there can be hyperechoic points with “comet-tail” artifacts corresponding to air in its interior. Likewise, they can present anechoic linear fistulous pathways which communicate the collection with the skin (Diaz, 2014).

Other sonographic findings of abscesses include hyperechoic sediment from necrotic debris, septa, loculations, posterior acoustic enhancement, and hyperechoic adjacent subcutaneous tissue. Gentle compression of the abscess with the transducer may show movement or ‘‘swirling’’ of purulent material (Adhikari and Blaivas, 2012).

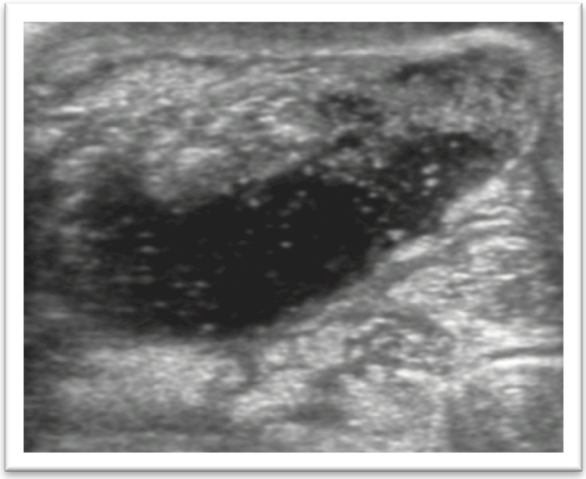

Fig. 18. Abscess with heterogeneous contents, including numerous tiny echoes representing gas bubbles. The tissues surrounding the abscess appear hyperechoic and disorganized secondary to inflammation (Figure adapted from Zwingerberger *et al*, 2015).

## *Pyoderma (bacterial folliculitis)*

Pyoderma is one of the most common diseases in dogs (Medleau and Hnilica, 2007).

Pyoderma literally means “pus in the skin” and can be caused by infectious, inflammatory, and/or neoplastic etiologies; any condition that results in the accumulation of neutrophilic exudate can be termed a pyoderma. Most commonly, however, pyoderma refers to bacterial infections of the skin. Superficial and deep pyoderma has been described (Summers *et al*, 2012).

In veterinary practice, the diagnosis of most cases of pyoderma is usually based upon clinical signs (hair loss, scaling, erythema) and the presence of characteristic lesions (papules, pustules, and epidermal collarettes) (Hillier *et al*, 2014).

Human are less prone to the development of pyoderma compared to dogs, as they possess a thicker stratum corneum, and their hair follicles are surrounded by a lipid plug (Lloyd and Garthwaite, 1982; Mason and Lloyd, 1993).

However, suppurative and inflammatory conditions of the skin have been described also in human literature, and US is currently used in the diagnosis of these conditions (Wortsman *et al*, 2012(a)).

For example, HFUS has been used in a condition called “Perifolliculitis capitis abscedens et suffodiens”, a severe dissecting folliculitis of the scalp, presenting with purulent-draining painful nodules, burrowing connecting tracts. In this case, HFUS shows debris-filled fluid collections and/or abscesses with multiple interconnecting hypoechoic fistulous tracts that reach the hair bulb, causing follicular swelling (Fig. 19) (Wortsman *et al*, 2012(a)).

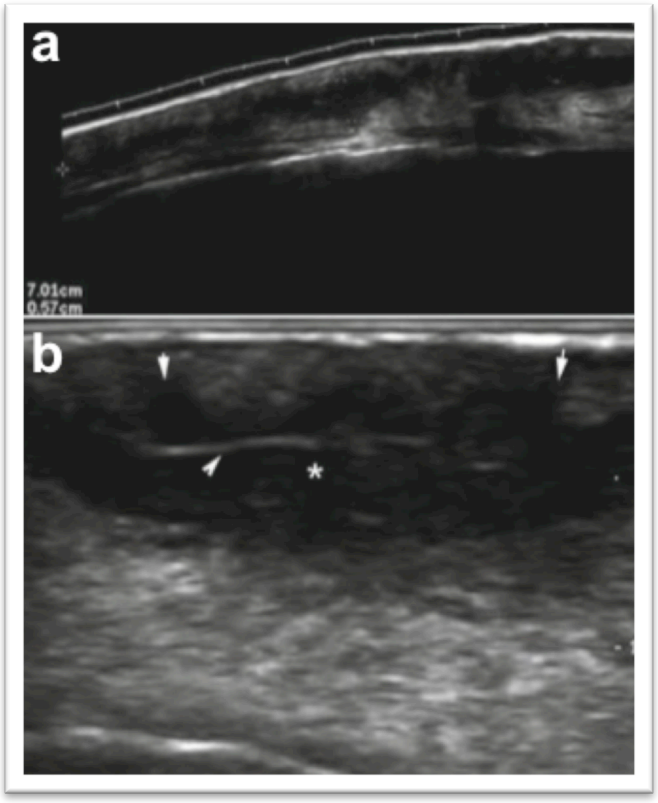


Fig. 19. US images of perifolliculitis of the scalp (capitis abscedens and suffodiens) in a man. a) Grey scale US image (longitudinal view) shows a 7 cm (long) x 0,57 cm (depth) anechoic fluid collection in the subcutaneous tissue. b) Transverse zoomed view presents hyperechoic lines that correspond to hair tract fragments (arrowheads) within the collection (asterisk). Notice the connecting tract (arrows) of the collection to the dermis (Figure adapted from Wortsman et al, 2012(a)).

## *Granuloma*

Granuloma is a special type of chronic inflammatory reaction that can be infectious or non-infectious in origin (Adhikari *et al*, 2012).

Foreign body granuloma is a tissue reaction for retained foreign bodies after skin-penetrating trauma and represents a common problem both in human and veterinary practice (Ando *et al*, 2009; Zwingerberger *et al*, 2015).

Depending on its nature, foreign bodies can be classified as inert (glass, metal, post-surgical

material) or organic (wood, bone fishes) (Wortsman, 2012; Diaz, 2014). Drugs may also act as "foreign bodies" and foreign body granuloma at site of injections has been described in both species (Fernandez-Flores *et al*, 2011; Yardimci *et al*, 2011).

US has been studied for detection and localization of foreign bodies and proved to be sensitive and specific in both human and veterinary medicine (Jacobson *et al*, 1998; Gnudi *et al*, 2005). When compared with MRI and CT, US is less expensive, readily available, and superior in the detection of foreign bodies (Ando *et al*, 2009).

The ultrasound enables to confirm the presence of a foreign body, the type of element and its exact location, which helps to extract the foreign body (Diaz, 2014).

The typical ultrasonographic appearance of a foreign body is a hyperechoic structure with distal acoustic shadowing (Fig. 20) (Shah *et al*, 1992; Matteucci *et al*, 1999; Armbrust *et al*, 2003).

Metallic foreign bodies may have a reverberating artifact within the distal shadow (Zwingenberger *et al*, 2015). Plant awn foreign bodies may produce or not distal shadowing, and may have a double or triple spindle shape on US (Gnudi *et al*, 2005).

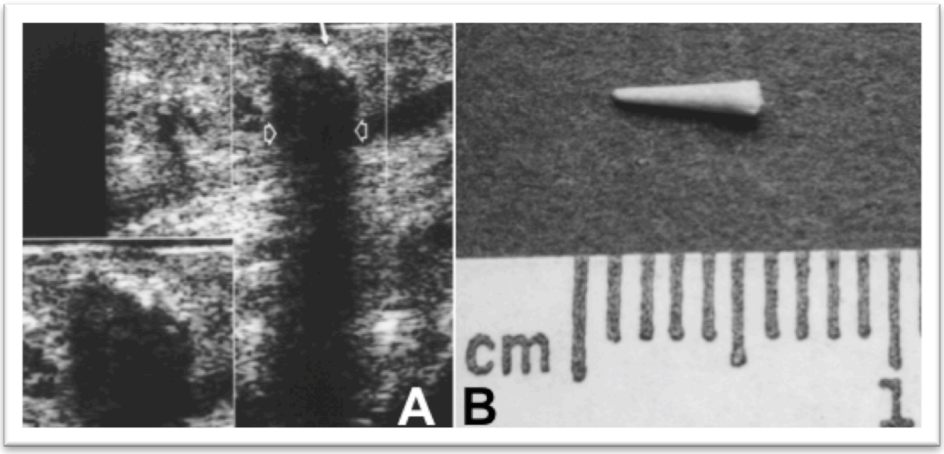


Fig. 20. (A) Sonogram of plantar surface of foot in a man reveals hyperechoic wooden toothpick (in long axis) (arrow). Note complete posterior acoustic shadowing (open arrows). Inset image is magnification view of foreign body. (B) 5-mm wooden toothpick fragment (Figure adapted from Horton *et al*, 2001).

Foreign bodies are often surrounded by hypoechoic halos which consist of reactive lesions such as hematoma, edema, fluid and granulation tissue (Shiels *et al*, 1990).

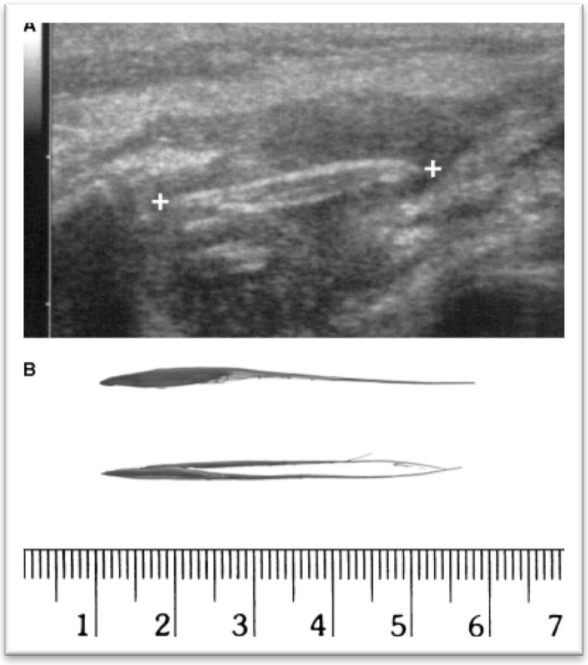


Fig. 21. (A) A grass awn is visible (between white callipers). Another partially visible grass awn is ventral to it. (B) The removed grass awns (Figure adapted from Gnudi *et al*, 2005).

By definition, foreign bodies within soft tissues are usually associated with "granuloma" formation (Joyce *et al*, 2014).

However, in case of foreign bodies providing a good medium for microbial agents, such as grass awns or pieces of wood, abscess and fistula formation may also develop (Chen and Sarma, 2014).

# PART III

## AIM OF THE STUDY

The aims of this study were to assess and document the spectrum of ultrasonographic features of superficial soft-tissue lesions in dogs and to evaluate the usefulness of high-resolution grayscale and Color Doppler ultrasound to distinguish benign from malignant soft-tissue masses on the basis of ultrasonographic patterns.

The final objective is to introduce HFUS in the diagnostic work-up of superficial soft-tissue lesions in dogs.

## MATERIALS AND METHODS

*INCLUSION CRITERIA*

***Animals***

Dogs that underwent high-resolution and color Doppler sonography of spontaneously-occurring cutaneous and subcutaneous lesions, as a part of daily clinical practice, during a 6-year period (January 2010 - December 2015) at the Veterinary Teaching Hospital of the University of Parma, Italy, were included.

***Imaging***

As Veterinary Teaching Hospital of Parma scanning protocol for superficial ultrasound lesions is standardised, all lesions included in this study were evaluated as follow:

- The skin surface was clipped and gently cleaned with chlorhexidine and 70% isopropyl alcohol to remove cutaneous debris and sebum;
- Copious amounts of coupling gel were applied between the transducer and skin surface. Gel Standoff pads were used in isolated case to obtain better images in case of lesions confined to epidermis or derma;
- Longitudinal and transverse scan were included;
- Doppler examination always followed B-mode examination. PRF and gain were adjusted according to the dimensions and deepness of the lesions;
- The ultrasound beam was maintained strictly perpendicular to the skin surface;
- Sonographic studies were conducted without sedation;
- 2 ultrasound machines (Esaote MyLab30Vet Gold (2010-2013) and Esaote Mylab ClassC, Genova, Italy (2014-2015)) equipped with broadband (frequency band, 10-12 MHz and 6-18 MHz) linear array transducers.

Only US examinations performed by one experienced operator of the teaching staff were included in the study.

***Image interpretations***

Two experienced radiologists reviewed retrospectively the digitized images without knowledge of clinical data, histologic results or the prospective sonographic report, in cooperation with one fellow. A final interpretation by consensus was given.

Each nodule was classified by measurement of fundamental sonographic parameters:

a. *Size* (minor and major diameter);

b. *Shape* (ovoid, round, polycyclic, irregular, spear-shape);

c. *Borders (margins)* (well or ill-defined);

Tumor margins were assessed as well-defined (clear-cut and thin capsule-like) and ill-defined (uncertain margin with respect to adjacent normal tissue).

d. *Echogenicity*;

The overall echogenicity was described as hyperechoic, hypoechoic or isoechoic relative to the surroundings cutaneous and subcutaneous tissue.

e. *Echotexture*;

Echotexture was classified as homogeneous (a consistent fine, grainy appearance throughout the mass) or heterogeneous (a coarse, irregular echotexture).

The classification of echotexture into homogeneous and heterogeneous is simplified, because in addition to these terms, texture can also be described by other adjectives such as fine or coarse.

f. *Acoustic shadowing or enhancement*

g. *Vascularity*

The CDUS appearance of each nodule was described:

•Semi-quantitatively (from 0 for no visible flow through 3 for extensive flow);

•Qualitatively (hilar, peripheral, capsular flow or combination of these).

***Pathology***

Only lesions that underwent aspiration cytology, biopsy, surgical debulking, ultrasound-guided

procedures or long-term clinical follow-up were included.

***Exclusion criteria***

Mammary tumors were not included in this study.

*STATISTICAL ANALYSIS*

All data regarding the clinical records were included in a database built using an Excel® sheet with the following variable fields: weight, sex, age, localization, lesion size, shape, borders, echogenicity, echotexture, acoustic enhancement, acoustic shadowing, CDUS and vessel distribution (hilar, peripheral or capsular).

The descriptive statistics, frequencies for catagorical variables (breed, sex, localization, shape, borders, echogenicity, echotexture, diagnosis and macrodiagnosis) and central tendency statistics for the quantitative continuous variable, were produced.

T-test was used to analyse the variables age, minor and major Diameter with regard to Macrodiagnosis levels.

The frequencies of counts for the categorical variables were analysed using Chi-square test (Yates corrected whenever appropriately) or Fisher's exact test for two by two tables, with respect to Macrodiagnosis and Diagnosis variables levels.

The variable Diagnosis was used in the analysis only considering the variable level having at least 5 counts (IC, MET, HPC, MCT, lipoma, abscess).

All the statistical analysis were conducted by using a commercial statistical software (IBM Corp. Released 2013. IBM SPSS Statistics for Windows, Version 22.0. Armonk, NY: IBM Corp) and the significance level was set for values of $P < 0.05$.

Statistical analysis was performed by a professional statistician.

# RESULTS

Data were obtained from 88 client-owned dogs (34 sexually intact males, 22 sexually intact females, 8 castrated male and 24 spayed female) that underwent high-resolution and color Doppler sonography for evaluation of spontaneously-occurring superficial soft-tissue nodules/masses (total of 107 lesions) during a 6-year period at the Veterinary Teaching Hospital of the University of Parma.

Dogs represented various breeds including 8 Labrador Retriever, 7 German Sheperd, 4 Boxer, 4 English Setters, 3 Rodesian Ridgeback, 3 Golden Retriever, 3 Dachshund, 2 Pinscher, 2 Dobermann, 2 Rottweiler, 2 French Bulldog, 2 English Bulldog, 2 Italian Hound, 2 Drahthaar, 1 Giant Schnauzer, 1 Toy Poodle, 1 Dogue de Bordeaux, 1 Bullmastiff, 1 Foxterrier, 1 Leonberger , 1 Cane Corso, 1 Samoiedo, 1 Belgian Sheperd; there were 33 mixed-breed dogs.

Dogs ranged from 3 months to 16 years of age (mean 8.3 ± 3,8) and from 5 to 63 Kg (mean, 24,3 ± 12). There were a total of 107 lesions, 54 were benign and 53 were malignant. Table 1 shows the distribution of benign lesions, and Table 2 shows the distribution of malignant lesions.

## Table 1. BENIGN SOFT-TISSUE LESIONS

| Lesions | (n) |
|---|---|
| EPYDERMAL INCLUSION CYST | 14 |
| LIPOMA | 12 |
| FOREIGN BODY ABSCESS | 11 |
| GRANULOMA | 4 |
| BENIGN CUTANEOUS HISTIOCYTOMA | 3 |
| FOLLICULAR NEOPLASIA | 3 |
| PYODERMITIS | 2 |
| HEPATOID GLANDS ADENOMA | 2 |
| STEATITIS | 1 |
| NODULAR DERMATOFIBROSIS | 1 |
| HEMANGIOMA | 1 |

## Table 2. MALIGNANT SOFT-TISSUE LESIONS

| Lesions | (n) |
|---|---|
| MAST CELL TUMORS | 38 |
| METASTASES | 7 |
| HEMANGIOPERICYTOMA | 5 |
| FIBROSARCOMA | 1 |
| CARCINOMA | 1 |
| MELANOMA | 1 |

Benign lesions included 22 benign neoplasia (12 lipomas, 3 benign histiocytoma, 3 follicular neoplasia, 2 hepatoid glands adenoma, 1 hemangioma, 1 nodular dermatofibrosis), 18 inflammatory lesions (11 foreign bodies abscesses, 4 granulomas, 2 pyodermitis, 1 steatitis) and 14 infundibular cysts.

Malignant lesions included: 38 mast cell tumors, 7 metastases, 5 hemangiopericytoma, 1 fibrosarcoma, 1 carcinoma and 1 melanoma.

Data collected are reported in table 3.

| ID | BREED | KG | SEX | AGE | LOCALIZATION | SIZE (cm) | SIZE 1 (major diameter) | SIZE 2 (minor diameter) | SHAPE | LESION BORDERS | ECHOGENICITY | ECHOTEXTURE | ACOUSTIC ENHANCEMENT | ACOUSTIC SHADOWING | CDUS | HILAR | PERIF | CAPS | CYTO | HISTO | DIAGNOSIS |
|---|---|---|---|---|---|---|---|---|---|---|---|---|---|---|---|---|---|---|---|---|---|
| 1 | BOXER | 30 | MI | 10 | NECK | 2,8 x 1,5 | 2,8 | 1,5 | OVOID | DEFINED | HYPO | HETEROGENEOUS | YES | NO | 0 | 0 | 0 | 0 | YES | YES | CYST |
| 2 | GIANT SCHNAUZER | 30 | FI | 8 | FLANK | 1,2 X 0,6 | 1,2 | 0,6 | OVOID | DEFINED | HYPO | HETEROGENEOUS | YES | NO | 0 | 0 | 0 | 0 | YES | YES | CYST |
| 3 | GIANT SCHNAUZER | 30 | FI | 8 | DORSUM | 1,2 X 0,6 | 1,2 | 0,6 | OVOID | DEFINED | HYPO | HETEROGENEOUS | YES | NO | 0 | 0 | 0 | 0 | YES | YES | CYST |
| 4 | GIANT SCHNAUZER | 30 | FI | 8 | DORSUM | 0,8 X 0,6 | 0,8 | 0,6 | OVOID | ILL-DEFINED | HYPO | HETEROGENEOUS | YES | NO | 1 | 0 | 1 | 0 | NO | NO | CYST |
| 5 | GIANT SCHNAUZER | 30 | FI | 8 | DORSUM | 2,2 X 1 | 2,2 | 1 | OVOID | DEFINED | HYPO | HETEROGENEOUS | YES | NO | 0 | 0 | 0 | 0 | YES | NO | CYST |
| 6 | CROSSBREED | 23 | FS | 6 | FLANK | 0,7 X 0,5 | 0,7 | 0,5 | ROUND | DEFINED | HYPO | HETEROGENEOUS | YES | NO | 0 | 0 | 0 | 0 | YES | YES | CYST |
| 7 | MINIATURE POODLE | 7,2 | FS | 9 | DORSUM | 1,8 X 0,4 | 1,8 | 0,4 | OVOID | DEFINED | HYPO | HETEROGENEOUS | YES | NO | 0 | 0 | 0 | 0 | YES | NO | CYST |
| 8 | MINIATURE POODLE | 7,2 | FS | 9 | DORSUM | 0,7 x 4,7 | 4,7 | 0,7 | OVOID | DEFINED | HYPO | HETEROGENEOUS | YES | NO | 0 | 0 | 0 | 0 | YES | NO | CYST |
| 9 | DRATHAR | 23 | FI | 6 | CHEST | 3,7 X 1,1 | 3,7 | 1,1 | OVOID | DEFINED | HYSO | HETEROGENEOUS | YES | NO | 0 | 0 | 0 | 0 | YES | NO | CYST |
| 10 | DOGUE DE BORDEAUX | 38 | FS | 11 | LIMB | 1,7 X 0,8 | 1,7 | 0,8 | OVOID | DEFINED | ISO | HETEROGENEOUS | NO | NO | 0 | 0 | 0 | 0 | YES | YES | CYST |
| 11 | CROSSBREED | 31 | MI | 13 | LIMB | 1,3 X 0,39 | 1,3 | 0,4 | OVOID | DEFINED | HYPO | HETEROGENEOUS | NO | NO | 0 | 0 | 0 | 0 | YES | YES | CYST |
| 12 | KURZHAAR | 31 | MI | 12 | CHEST | 2,4 X 0,5 | 2,4 | 0,5 | OVOID | ILL-DEFINED | HYPO | HETEROGENEOUS | NO | NO | 0 | 0 | 0 | 0 | YES | NO | CYST |
| 13 | BULL MASTIFF | 48 | FI | 4 | LIMB | 0,9 X 0,3 | 0,9 | 0,3 | OVOID | DEFINED | HYPO | HETEROGENEOUS | YES | NO | 0 | 0 | 0 | 0 | YES | NO | CYST |
| 14 | BULL MASTIFF | 48 | FI | 4 | LIMB | 0,4 X 0,2 | 0,4 | 0,2 | OVOID | DEFINED | HYPO | HETEROGENEOUS | YES | NO | 0 | 0 | 0 | 0 | YES | NO | CYST |
| 15 | CROSSBREED | 15 | MI | 13 | LIMB | 2,6 X 1,7 | 2,6 | 1,7 | POLYCYCLIC | DEFINED | HYPO | HOMOGENEOUS | NO | YES | 3 | 1 | 1 | 0 | NO | YES | MET |
| 16 | CROSSBREED | 25 | FS | 12 | CHEST | 1,1 x 1,2 | 1,2 | 1,1 | POLYCYCLIC | DEFINED | HYPO | HOMOGENEOUS | YES | NO | 3 | 1 | 1 | 0 | YES | YES | MET |
| 17 | GOLDEN RETRIEVER | 30 | FI | 12 | LIMB | 1,5 x 1,5 | 1,5 | 1,5 | POLYCYCLIC | DEFINED | HYPO | HOMOGENEOUS | YES | NO | 3 | 1 | 1 | 0 | NO | YES | MET |
| 18 | GERMAN SHEPERD | 43 | MC | 10 | ABDOMEN | 2 X 1 | 2 | 1 | POLYCYCLIC | DEFINED | HYPO | HOMOGENEOUS | YES | NO | 3 | 1 | 1 | 0 | YES | NO | MET |
| 19 | DACHSHUND | 7,5 | FI | 12 | LIMB | 0,9 X 0,3 | 0,9 | 0,3 | POLYCYCLIC | DEFINED | HYPO | HOMOGENEOUS | YES | NO | 2 | 0 | 1 | 0 | NO | NO | MET |
| 20 | RODESIAN RIDGEBACK | 50 | MC | 13 | LIMB | 2,3 X 1,5 | 2,3 | 1,5 | POLYCYCLIC | DEFINED | HYPO | HOMOGENEOUS | YES | NO | 3 | 1 | 1 | 0 | YES | NO | MET |
| 21 | ROTTWEILER | 41 | FI | 10 | CHEST | 1,2 x 2,0 | 2 | 1,2 | POLYCYCLIC | ILL-DEFINED | HYPO | HOMOGENEOUS | NO | NO | 3 | 1 | 1 | 0 | YES | NO | MET |

| | | | | | | | | | | | | | | | | | | | | |
|---|---|---|---|---|---|---|---|---|---|---|---|---|---|---|---|---|---|---|---|---|
| 22 | CROSSBREED | 6,5 | MI | 1 | LIMB | 1,2 X 0,5 | 1,2 | 0,5 | OVOID | DEFINED | ISO | HOMOGENEOUS | YES | NO | 1 | 0 | 0 | 1 | YES | NO | CH |
| 23 | GERMAN SHEPERD | 39 | MI | 6 | LIMB | 1,5 X 0,6 | 1,5 | 0,6 | OVOID | DEFINED | ISO | HOMOGENEOUS | NO | NO | 1 | 0 | 0 | 1 | YES | NO | CH |
| 24 | CROSSBREED | 24 | MI | 10 | HEAD | 0,8 x 0,5 | 0,8 | 0,5 | OVOID | DEFINED | ISO | HOMOGENEOUS | NO | NO | 1 | 0 | 1 | 1 | YES | YES | CH |
| 25 | CROSSBREED | 12 | MI | 15 | LIMB | 1,9 X 1,4 | 1,9 | 1,4 | OVOID | ILL-DEFINED | HYPO | HETEROGENEOUS | NO | NO | 3 | 1 | 1 | 1 | YES | NO | HPC |
| 26 | CROSSBREED | 36 | MI | 9 | LIMB | 2,8 X 1 | 2,8 | 1 | OVOID | ILL-DEFINED | HYPO | HETEROGENEOUS | NO | NO | 3 | 1 | 1 | 0 | YES | NO | HPC |
| 27 | LABRADOR RETRIEVER | 37 | MI | 10 | LIMB | 2,8 X 0,7 | 2,8 | 0,7 | OVOID | ILL-DEFINED | HYPO | HETEROGENEOUS | NO | NO | 3 | 1 | 1 | 1 | YES | YES | HPC |
| 28 | CROSSBREED | 21 | MI | 6 | LIMB | 1,8 X 3 | 3 | 1,8 | OVOID | ILL-DEFINED | HYPO | HETEROGENEOUS | NO | NO | 2 | 1 | 1 | 0 | NO | YES | HPC |
| 29 | CROSSBREED | 15 | FS | 15 | LIMB | 3,8 X 2,4 | 3,8 | 2,4 | OVOID | ILL-DEFINED | HYPO | HETEROGENEOUS | NO | NO | 3 | 1 | 1 | 1 | YES | YES | HPC |
| 30 | CROSSBREED | 15 | MI | 14 | LIMB | 2,1 x 0,6 | 2,1 | 0,6 | OVOID | DEFINED | ISO | HETEROGENEOUS | NO | NO | 0 | 0 | 0 | 0 | YES | NO | MCT |
| 31 | ROTTWEILER | 41 | FI | 9 | LIMB | 4,7 X 4,6 | 4,7 | 4,6 | ROUND | ILL-DEFINED | HYPO | HETEROGENEOUS | NO | NO | 3 | 1 | 1 | 1 | YES | YES | MCT |
| 32 | RODESIAN RIDGEBACK | 30 | MI | 10 | LIMB | 2,7 X 0,9 | 2,7 | 0,9 | OVOID | DEFINED | ISO | HOMOGENEOUS | NO | NO | 1 | 0 | 0 | 1 | YES | YES | MCT |
| 33 | RODESIAN RIDGEBACK | 30 | MI | 10 | LIMB | 2,2 X 0,7 | 2,2 | 0,7 | OVOID | DEFINED | ISO | HETEROGENEOUS | YES | YES | 0 | 0 | 0 | 0 | YES | NO | MCT |
| 34 | CROSSBREED | 15 | MI | 5 | CHEST | 1,9 X 0,5 | 1,9 | 0,5 | SPEAR-SHAPE | DEFINED | HYPO | HOMOGENEOUS | NO | NO | 0 | 0 | 0 | 0 | YES | NO | MCT |
| 35 | CROSSBREED | 8 | FS | 11 | LIMB | 2,6 X0,8 | 2,6 | 0,8 | SPEAR-SHAPE | DEFINED | ISO | HOMOGENEOUS | NO | NO | 2 | 1 | 1 | 1 | YES | YES | MCT |
| 36 | ENGLISH SETTER | 19 | FI | 9 | CHEST | 2,7 X1 | 2,7 | 1 | SPEAR-SHAPE | DEFINED | HYPO | HOMOGENEOUS | NO | NO | 2 | 1 | 0 | 1 | YES | NO | MCT |
| 37 | ENGLISH SETTER | 19 | FI | 9 | LIMB | 2,3 X 0,7 | 2,3 | 0,7 | SPEAR-SHAPE | DEFINED | HYPO | HOMOGENEOUS | NO | NO | 1 | 0 | 0 | 1 | YES | NO | MCT |
| 38 | ENGLISH SETTER | 20 | FI | 8 | DORSUM | 1,1X0,6 | 1,1 | 0,6 | OVOID | DEFINED | ISO | HETEROGENEOUS | YES | NO | 1 | 1 | 0 | 1 | YES | NO | MCT |
| 39 | RODESIAN RIDGEBACK | 36 | FI | 5 | LIMB | 1,6 X 0,5 | 1,6 | 0,5 | SPEAR-SHAPE | DEFINED | ISO | HETEROGENEOUS | NO | NO | 1 | 0 | 0 | 1 | YES | YES | MCT |
| 40 | CROSSBREED | 16 | MI | 7 | LIMB | 4,5 X 2,9 | 4,5 | 2,9 | OVOID | ILL-DEFINED | HYPO | HETEROGENEOUS | NO | NO | 3 | 1 | 1 | 0 | YES | NO | MCT |
| 41 | CROSSBREED | 25 | FS | 2 | LIMB | 1,6 X 0,47 | 1,6 | 0,5 | SPEAR-SHAPE | DEFINED | ISO | HOMOGENEOUS | NO | NO | 2 | 1 | 1 | 1 | YES | NO | MCT |
| 42 | BOXER | 24 | FI | 6 | LIMB | 4,4 X 0,9 | 4,4 | 0,9 | OVOID | ILL-DEFINED | HYPO | HETEROGENEOUS | NO | NO | 3 | 1 | 0 | 1 | YES | NO | MCT |
| 43 | PINSCHER | 5 | MI | 8 | LIMB | 1,5 x 0,5 | 1,5 | 0,5 | SPEAR-SHAPE | DEFINED | ISO | HOMOGENEOUS | YES | NO | 3 | 1 | 1 | 1 | YES | YES | MCT |

| | | | | | | | | | | | | | | | | | | | | |
|---|---|---|---|---|---|---|---|---|---|---|---|---|---|---|---|---|---|---|---|---|
| 44 | PINSCHER | 5,5 | FI | 7 | LIMB | 1,6 X 0,4 | 1,6 | 0,4 | SPEAR-SHAPE | ILL-DEFINED | HYPO | HETEROGENEOUS | NO | NO | 1 | 0 | 0 | 1 | YES | YES | MCT |
| 45 | CROSSBREED | 7 | FI | 13 | LIMB | 2 x 0,5 | 2 | 0,5 | OVOID | ILL-DEFINED | HYPO | HETEROGENEOUS | NO | NO | 1 | 0 | 0 | 1 | YES | YES | MCT |
| 46 | CROSSBREED | 20 | MI | 5 | LIMB | 2,8 X 1 | 2,8 | 1 | OVOID | DEFINED | ISO | HOMOGENEOUS | NO | NO | 1 | 0 | 0 | 1 | YES | YES | MCT |
| 47 | LABRADOR RETRIEVER | 33 | MI | 11 | LIMB | 3,7 X 0,8 | 3,7 | 0,8 | OVOID | ILL-DEFINED | ISO | HETEROGENEOUS | NO | NO | 1 | 0 | 0 | 1 | YES | NO | MCT |
| 48 | CROSSBREED | 15 | FS | 9 | CHEST | 1,5 X 0,5 | 1,5 | 0,5 | OVOID | DEFINED | HYPO | HOMOGENEOUS | NO | NO | 1 | 0 | 0 | 1 | YES | YES | MCT |
| 49 | LABRADOR RETRIEVER | 37 | FS | 11 | LIMB | 1,1 X 0,6 | 1,1 | 0,6 | SPEAR-SHAPE | DEFINED | ISO | HOMOGENEOUS | YES | NO | 1 | 0 | 0 | 1 | YES | YES | MCT |
| 50 | CROSSBREED | 7 | FS | 8 | LIMB | 4 X 5 | 5 | 4 | ROUND | ILL-DEFINED | HYPO | HETEROGENEOUS | NO | NO | 3 | 1 | 1 | 1 | YES | NO | MCT |
| 51 | LABRADOR RETRIEVER | 30 | FS | 9 | LIMB | 2,5 X 0,4 | 2,5 | 0,4 | OVOID | DEFINED | HYPO | HETEROGENEOUS | NO | NO | 1 | 0 | 0 | 1 | YES | NO | MCT |
| 52 | CROSSBREED | 25 | MC | 8 | DORSUM | 3,7 X 1,2 | 3,7 | 1,2 | SPEAR-SHAPE | DEFINED | ISO | HETEROGENEOUS | NO | NO | 3 | 1 | 1 | 1 | YES | NO | MCT |
| 53 | FRENCH BULLDOG | 10 | MI | 11 | SCROTUM | 3,5 X 4,5 | 4,5 | 3,5 | OVOID | ILL-DEFINED | HYPER | HETEROGENEOUS | NO | NO | 3 | 1 | 1 | 1 | YES | YES | MCT |
| 54 | LABRADOR RETRIEVER | 30 | MI | 13 | LIMB | 1,8 X 0,6 | 1,8 | 0,6 | SPEAR-SHAPE | DEFINED | HYPO | HOMOGENEOUS | NO | NO | 1 | 0 | 0 | 1 | YES | NO | MCT |
| 55 | BOXER | 25 | FS | 9 | LIMB | 2,3 X 1,2 | 2,3 | 1,2 | SPEAR-SHAPE | DEFINED | ISO | HETEROGENEOUS | NO | NO | 2 | 0 | 0 | 1 | YES | NO | MCT |
| 56 | ENGLISH BULLDOG | 25 | MC | 8 | NECK | 1,7 X 1,4 | 1,7 | 1,4 | SPEAR-SHAPE | DEFINED | ISO | HETEROGENEOUS | NO | NO | 0 | 0 | 0 | 0 | YES | NO | MCT |
| 57 | GOLDEN RETRIEVER | 32 | MI | 8 | NECK | 2,5 X 0,8 | 2,5 | 0,8 | SPEAR-SHAPE | DEFINED | ISO | HOMOGENEOUS | NO | NO | 1 | 0 | 0 | 1 | YES | NO | MCT |
| 58 | CROSSBREED | 15 | MI | 11 | LIMB | 4,7 X 2,7 | 4,7 | 2,7 | ROUND | ILL-DEFINED | ISO | HETEROGENEOUS | NO | NO | 2 | 1 | 1 | 1 | YES | NO | MCT |
| 59 | ITALIAN HOUND | 22 | FS | 11 | CHEST | 5,3 X 2,9 | 5,3 | 2,9 | OVOID | DEFINED | HYPO | HOMOGENEOUS | NO | NO | 3 | 1 | 1 | 1 | | YES | MCT |
| 60 | CROSSBREED | 32 | MI | 8 | CHEST | 1,5 X 0,4 | 1,5 | 0,4 | OVOID | DEFINED | HYPO | HOMOGENEOUS | NO | NO | 0 | 0 | 0 | 0 | YES | YES | MCT |
| 61 | GOLDEN RETRIEVER | 35 | MI | 6 | FLANK | 2 X 0,7 | 2 | 0,7 | SPEAR-SHAPE | DEFINED | ISO | HOMOGENEOUS | NO | NO | 2 | 1 | 0 | 1 | YES | NO | MCT |
| 62 | BOXER | 23 | FS | 6 | LIMB | 3,1 X 2,4 | 3,1 | 2,4 | SPEAR-SHAPE | ILL-DEFINED | ISO | HOMOGENEOUS | NO | NO | 1 | 0 | 0 | 1 | YES | NO | MCT |
| 63 | CROSSBREED | 13 | FS | 8 | ABDOMEN | 1,7 X 0,5 | 1,7 | 0,5 | SPEAR-SHAPE | ILL-DEFINED | ISO | HOMOGENEOUS | NO | NO | 1 | 0 | 0 | 1 | YES | NO | MCT |
| 64 | CROSSBREED | 13 | FS | 8 | LIMB | 2,2 X 0,7 | 2,2 | 0,7 | SPEAR-SHAPE | DEFINED | ISO | HOMOGENEOUS | NO | NO | 1 | 0 | 0 | 1 | YES | NO | MCT |
| 65 | CROSSBREED | 13 | FS | 8 | LIMB | 4 X 1 | 4 | 1 | OVOID | DEFINED | ISO | HETEROGENEOUS | NO | NO | 3 | 0 | 1 | 1 | YES | NO | MCT |
| 66 | CROSSBREED | 25 | MI | 16 | CHEST | 1,7 X 0,6 | 1,7 | 0,6 | SPEAR-SHAPE | DEFINED | HYPO | HOMOGENEOUS | NO | NO | 1 | 0 | 0 | 1 | YES | NO | MCT |
| 67 | ENGLISH SETTER | 23 | MI | 12 | ABDOMEN | 2,5 X 0,6 | 2,5 | 0,6 | SPEAR-SHAPE | DEFINED | ISO | HOMOGENEOUS | NO | NO | 3 | 1 | 0 | 1 | YES | NO | MCT |

| | | | | | | | | | | | | | | | | | | | | |
|---|---|---|---|---|---|---|---|---|---|---|---|---|---|---|---|---|---|---|---|---|
| 68 | RODESIAN RIDGEBACK | 36 | FI | 5 | STERNUM | 1,7 X 0,5 | 1,7 | 0,5 | OVOID | DEFINED | ISO | HETEROGENEOUS | NO | NO | 0 | 0 | 0 | 0 | YES | NO | LIPOMA |
| 69 | CROSSBREED | 15 | FS | 10 | LIMB | 3,5 X 1,6 | 3,5 | 1,6 | OVOID | DEFINED | ISO | HETEROGENEOUS | NO | NO | 0 | 0 | 0 | 0 | YES | NO | LIPOMA |
| 70 | KURZHAAR | 31 | MI | 12 | STERNUM | 2,9 x 0,7 | 2,9 | 0,7 | OVOID | DEFINED | ISO | HETEROGENEOUS | NO | NO | 1 | 0 | 1 | 0 | YES | NO | LIPOMA |
| 71 | CROSSBREED | 8 | FS | 14 | FLANK | 3,8 x 0,8 | 3,8 | 0,8 | OVOID | DEFINED | HYPO | HETEROGENEOUS | NO | NO | 0 | 0 | 0 | 0 | YES | NO | LIPOMA |
| 72 | GERMAN SHEPERD | 31 | FI | 8 | LIMB | 3 X 1,1 | 3 | 1,1 | OVOID | DEFINED | HYPO | HETEROGENEOUS | NO | NO | 0 | 0 | 0 | 0 | YES | NO | LIPOMA |
| 73 | LABRADOR RETRIEVER | 37 | FS | 11 | LIMB | 2,8 X 0,7 | 2,8 | 0,7 | OVOID | DEFINED | HYPO | HETEROGENEOUS | NO | NO | 0 | 0 | 0 | 0 | YES | YES | LIPOMA |
| 74 | CROSSBREED | 10 | FS | 10 | ABDOMEN | 1,8 x 0,6 | 1,8 | 0,6 | OVOID | DEFINED | ISO | HETEROGENEOUS | NO | NO | 0 | 0 | 0 | 0 | YES | NO | LIPOMA |
| 75 | CROSSBREED | 15 | MC | 15 | DORSUM | 2,9 x 1 | 2,9 | 1 | OVOID | DEFINED | ISO | HETEROGENEOUS | NO | NO | 0 | 0 | 0 | 0 | YES | NO | LIPOMA |
| 76 | LABRADOR RETRIEVER | 33 | MC | 12 | NECK | 4 x 2 | 4 | 2 | OVOID | DEFINED | HYPO | HETEROGENEOUS | NO | NO | 0 | 0 | 0 | 0 | YES | NO | LIPOMA |
| 77 | CROSSBREED | 8 | FS | 15 | NECK | 7 x 8 | 8 | 7 | OVOID | DEFINED | ISO | HETEROGENEOUS | NO | NO | 0 | 0 | 0 | 0 | YES | YES | LIPOMA |
| 78 | ROTTWEILER | 46 | FS | 11 | ABDOMEN | 4,6 x 3 | 4,6 | 3 | OVOID | DEFINED | ISO | HETEROGENEOUS | NO | NO | 0 | 0 | 0 | 0 | YES | NO | LIPOMA |
| 79 | LABRADOR RETRIEVER | 35 | FS | 10 | LIMB | 2,8 x 0,8 | 2,8 | 0,8 | OVOID | DEFINED | HYPO | HETEROGENEOUS | NO | NO | 0 | 0 | 0 | 0 | YES | NO | LIPOMA |
| 80 | CROSSBREED | 15 | FS | 1 | LIMB | 3 x 1,3 | 3 | 1,3 | OVOID | ILL-DEFINED | ISO | HETEROGENEOUS | NO | NO | 1 | 0 | 1 | 0 | NO | NO | ABSCESS |
| 81 | CROSSBREED | 15 | FS | 1 | LIMB | 2,3 X 0,6 | 2,3 | 0,6 | OVOID | ILL-DEFINED | ISO | HETEROGENEOUS | NO | NO | 3 | 1 | 0 | 1 | NO | NO | ABSCESS |
| 82 | ENGLISH SETTER | 15 | FS | 1 | CHEST | 2,8 x 1 | 2,8 | 1 | IRREGULAR | ILL-DEFINED | ISO | HOMOGENEOUS | NO | YES | 0 | 0 | 0 | 0 | NO | NO | ABSCESS |
| 83 | CROSSBREED | 26 | MI | 6 | CHEST | 4,5 x 1,8 | 4,5 | 1,8 | OVOID | ILL-DEFINED | HYPO | HETEROGENEOUS | NO | YES | 1 | 0 | 1 | 0 | NO | NO | ABSCESS |
| 84 | KURZHAAR | 20 | FS | 3 | CHEST | 2,7 x 1,9 | 2,7 | 1,9 | IRREGULAR | ILL-DEFINED | HYPO | HOMOGENEOUS | NO | YES | 1 | 0 | 1 | 0 | NO | NO | ABSCESS |
| 85 | SAMOIEDO | 20 | FI | 12 | STERNUM | 3,7 x 0,8 | 3,7 | 0,8 | IRREGULAR | DEFINED | HYPO | HOMOGENEOUS | YES | YES | 0 | 0 | 0 | 0 | NO | NO | ABSCESS |
| 86 | ENGLISH BULLDOG | 28 | MC | 1 | NECK | 4,4 x 2,4 | 4,4 | 2,4 | IRREGULAR | ILL-DEFINED | HYPO | HETEROGENEOUS | NO | YES | 0 | 0 | 0 | 0 | YES | NO | ABSCESS |
| 87 | FOX TERRIER | 10 | FI | 4 | LIMB | 3,8 x 0,7 | 3,8 | 0,7 | IRREGULAR | DEFINED | ISO | HETEROGENEOUS | NO | YES | 0 | 0 | 0 | 0 | NO | NO | ABSCESS |
| 88 | ITALIAN HOUND | 8 | FS | 0 | LIMB | 3,3 x 0,9 | 3,3 | 0,9 | OVOID | DEFINED | ISO | HETEROGENEOUS | NO | YES | 0 | 0 | 0 | 0 | NO | NO | ABSCESS |
| 89 | LEONBERGER | 63 | FI | 3 | CHEST | 4 X 4 | 4 | 4 | OVOID | ILL-DEFINED | HYPO | HETEROGENEOUS | NO | NO | 0 | 0 | 0 | 0 | NO | NO | ABSCESS |
| 90 | BELGIAN SHEPERD | 13 | MI | 0 | DORSUM | 2,3 x 1,9 | 2,3 | 1,9 | IRREGULAR | ILL-DEFINED | HYPO | HETEROGENEOUS | NO | YES | 1 | 0 | 1 | 0 | NO | NO | ABSCESS |

| | | | | | | | | | | | | | | | | | | | | | | | |
|---|---|---|---|---|---|---|---|---|---|---|---|---|---|---|---|---|---|---|---|---|---|---|---|
| 92 | CROSSBREED | 24 | MI | 10 | DORSUM | 3,9 X 2,6 | 3,9 | 2,6 | OVOID | DEFINED | HYPO | HETEROGENEOUS | NO | NO | 0 | 0 | 0 | 0 | YES | NO | GRANULOMA |
| 93 | CORSO | 35 | FS | 2 | DORSUM | 3 X 1,5 | 3 | 1,5 | OVOID | DEFINED | HYPO | HETEROGENEOUS | NO | NO | 1 | 0 | 0 | 0 | NO | YES | GRANULOMA |
| 94 | DOBERMANN | 35 | FI | 2 | LIMB | 1,7 X 0,5 | 1,7 | 0,5 | OVOID | ILL-DEFINED | ISO | HOMOGENEOUS | NO | NO | 3 | 1 | 1 | 1 | YES | NO | GRANULOMA |
| 95 | LABRADOR RETRIEVER | 20 | FI | 1 | DORSUM | 3 X 0,5 | 3 | 0,5 | OVOID | ILL-DEFINED | HYPO | HETEROGENEOUS | NO | NO | 0 | 0 | 0 | 0 | YES | NO | GRANULOMA |
| 96 | GERMAN SHEPERD | 36 | MI | 7 | LIMB | 2,8 X 0,6 | 2,8 | 0,6 | OVOID | ILL-DEFINED | HYPER | HETEROGENEOUS | NO | NO | 3 | 0 | 1 | 0 | NO | NO | PYODERMITIS |
| 97 | CROSSBREED | 20 | MI | 5 | LIMB | 2,8 X 0,6 | 2,8 | 0,6 | OVOID | ILL-DEFINED | HYPER | HETEROGENEOUS | NO | NO | 3 | 1 | 1 | 0 | NO | YES | PYODERMITIS |
| 98 | LABRADOR RETRIEVER | 37 | FS | 11 | LIMB | 2,2 X 0,7 | 2,2 | 0,7 | OVOID | ILL-DEFINED | ISO | HETEROGENEOUS | NO | NO | 0 | 0 | 0 | 0 | NO | YES | STEATITIS |
| 99 | GERMAN SHEPERD | 33 | FI | 6 | DORSUM | 3,7 x 1,2 | 3,7 | 1,2 | OVOID | DEFINED | HYPER | HETEROGENEOUS | NO | NO | 0 | 0 | 0 | 0 | NO | YES | FOLLICULAR NEOPLASIA |
| 100 | GERMAN SHEPERD | 35 | FI | 10 | LIMB | 2 x 0,9 | 2 | 0,9 | OVOID | DEFINED | ISO | HOMOGENEOUS | NO | YES | 3 | 1 | 1 | 1 | NO | NO | NODULAR DERMATOFIBROSIS |
| 101 | CROSSBREED | 20 | FI | 6 | LIMB | 1 X 0,5 cm | 1 | 0,5 | OVOID | DEFINED | HYPO | HOMOGENEOUS | NO | NO | 1 | 0 | 1 | 1 | YES | NO | FOLLICULAR NEOPLASIA |
| 102 | GERMAN SHEPERD | 45 | MI | 14 | DORSUM | 2,8 x 1,5 | 2,8 | 1,5 | OVOID | ILL-DEFINED | HYPO | HETEROGENEOUS | YES | NO | 3 | 1 | 1 | 0 | YES | NO | FOLLICULAR NEOPLASIA |
| 103 | DACHSHUND | 6,5 | MI | 12 | PERIANAL | 1,1 X 0,7 | 1,1 | 0,7 | ROUND | DEFINED | HYPO | HETEROGENEOUS | NO | NO | 3 | 1 | 1 | 0 | YES | NO | ADENOMA |
| 104 | DACHSHUND | 6 | MI | 4 | LIMB | 1,1 X 0,7 | 1,1 | 0,7 | OVOID | DEFINED | HYPO | HETEROGENEOUS | YES | NO | 1 | 0 | 1 | 0 | YES | YES | HEMANGIOMA |
| 105 | CROSSBREED | 10 | MI | 11 | DORSUM | 2,8 x 0,9 | 2,8 | 0,9 | OVOID | DEFINED | HYPO | HETEROGENEOUS | YES | NO | 2 | 1 | 1 | 1 | YES | NO | ADENOMA |
| 106 | FRENCH BULLDOG | 10 | MC | 11 | HEAD | 0,8 X 0,7 | 0,8 | 0,7 | POLYCYCLIC | ILL-DEFINED | HYPO | HOMOGENEOUS | YES | NO | 3 | 1 | 1 | 1 | NO | YES | MELANOMA |
| 107 | DOBERMANN | 33 | FS | 10 | LIMB | 2 X 1 | 2 | 1 | OVOID | ILL-DEFINED | HYPO | HOMOGENEOUS | NO | NO | 3 | 1 | 1 | 1 | YES | YES | FIBROSARCOMA |
| 108 | LABRADOR RETRIEVER | 33 | MI | 3 | DORSUM | 1,2 x 0,8 | 1,2 | 0,8 | POLYCYCLIC | ILL-DEFINED | HYPO | HOMOGENEOUS | YES | NO | 2 | 0 | 0 | 1 | YES | YES | CARCINOMA |

**Table 3**. Clinical information associated with histologic, sonographic, and Color Doppler parameters of the lesions.

## BENIGN LESIONS

### INFUNDIBULAR CYST (14)

US showed that the epydermal inclusion cysts presented as hypoechoic, heterogeneous solid-appearing lesions in 14 cases (100%). 10 lesions (71,4%) showed internal hyperechoic bright striations. Of these 10 lesions, 4 displayed specific patterns, borrowed by human medicine: an onion ring pattern (concentric hyperechoic and hypoechoic rings) (Fig. 22) in two cases, a tram track pattern (Fig. 23) in one case and a pseudotestis pattern (Fig. 24) in one case.

The margins were well-defined in 12 (85,7%) lesions and shape was oval in 13 (76 %). The longest diameter (size) ranged from 0,4 to 4,7 cm (mean, 1,84 cm). Acoustic enhancement was present in 11 (78,5%). 13 lesions (92,8%) were grade 0 on CDUS. Only 1 lesion (7,1%) showed peripheral vascular flow. 5 lesions (35,7%) were located along the dorsal midline.

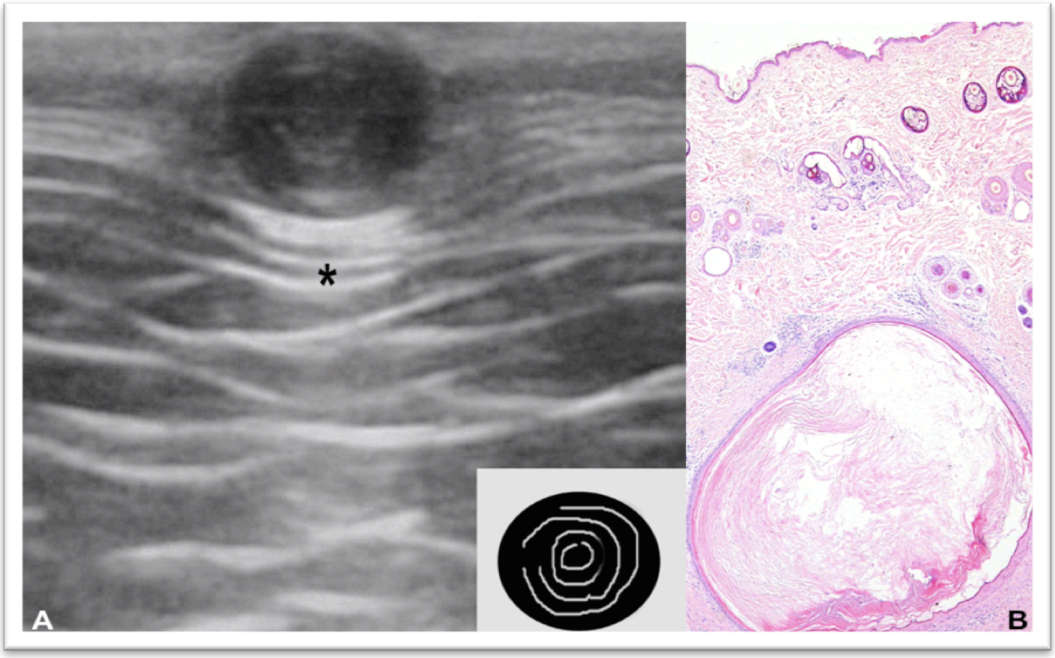


**Fig. 22. Dog, case 6.** (A) US longitudinal image of an infundibular cyst in a 6-year-old, spayed female cross-breed dog, showing a 0.7 cm wide, well-encapsulated and heterogeneously hypoechoic nodule with alternating hypoechoic and hyperechoic concentric rings which looks like an onion ring. Moderate through-transmission is shown (asterisk). The corresponding schematic drawing is shown in the lower panel. (B) Photomicrograph. Infundibular cyst in the deep dermis/subcutis containing layers of lamellar keratin, concentrically arranged (Haematoxylin and Eosin (H&E) staining), which correspond to the onion ring pattern on US.

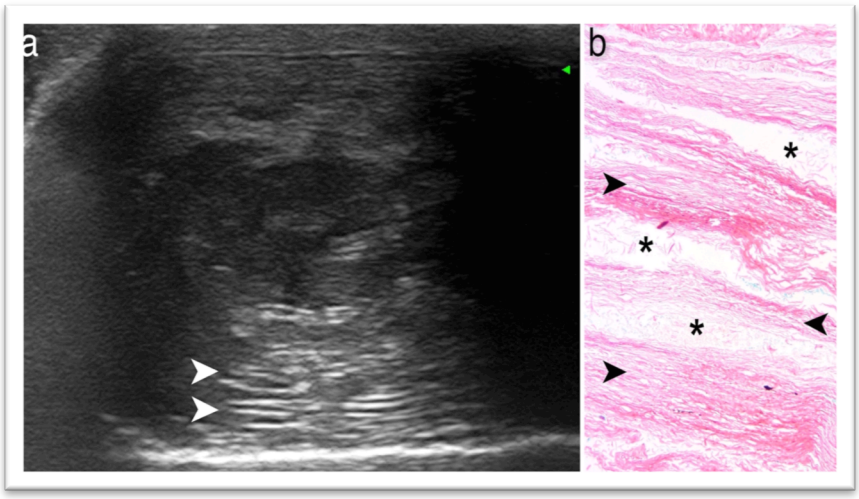


**Fig. 23. Dog, case 1.** Comparison of skin nodule ultrasound and histological findings in a 10 year-old, entire male, Boxer dog. (a) US longitudinal image showing a well encapsulated heteroechoic nodule, about 2,8 cm wide. The nodule reveals multiple parallel alternating hyperechoic and hypoechoic lines (white arrowheads) suggestive of a tram-track. (b) Pathologic specimen showing multiple layers of compact laminae (Haematoxylin and Eosin (H&E) staining). Aggregated and layered keratin debris (arrowheads) is responsible for the hyperechoic lines seen on US, while the hypoechoic lines occur in areas lacking keratins (asterisks).

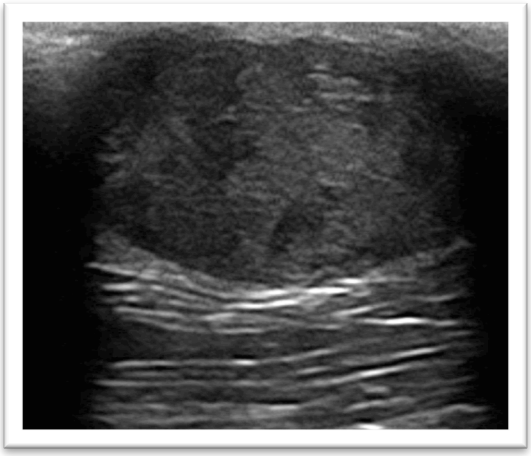

**Fig. 24. Dog, case 5.** US longitudinal image of an infundibular cyst in a 8-year-old, entire female, Giant Schnauzer, showing a 2,2 cm wide, well-marginated and heterogeneously hypoechoic nodule. A pseudotestis pattern is shown.

LIPOMA (12)

There were 12 lipomas, all (100%) were oval and had well-defined margins. They all (100%) were heterogeneous in echotexture, with multiple hyperechoic parallel stripes along the major axis of the lesion (Fig. 25). The longest diameter (size) ranged from 1,7 to 4,6 cm (mean, 3,5). 7 lipomas (58,3%) were isoechoic to the surrounding tissues, 5 (41,7%) hypoechoic. 11 (91,7%) were avascular. On CDUS, 11 lipomas were classified as grade 0. Four lipomas (33,3%) were located in the extremities, the remaining 8 were located in the trunk.

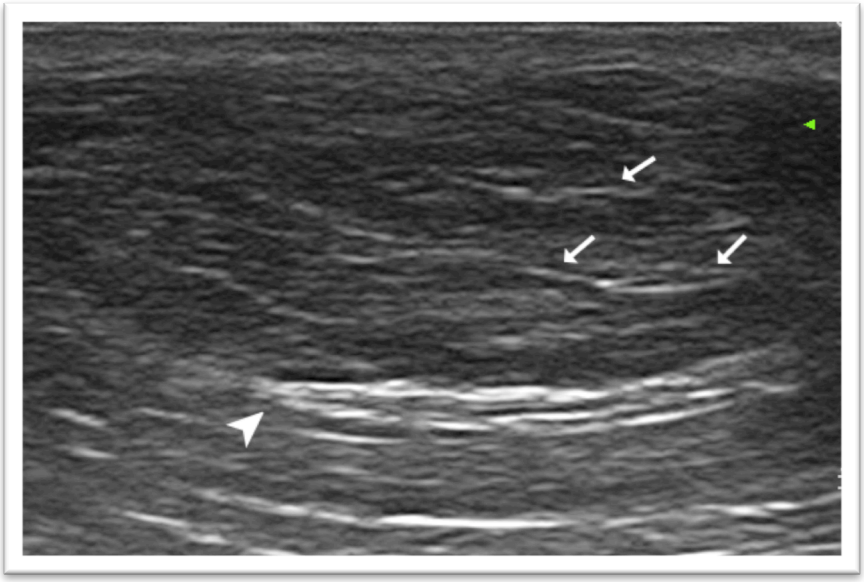

**Fig. 25. Dog, case 71**. Ultrasonographic image of a lipoma of the flank region in a 14-year-old, spayed female, cross-breed dog. An ovalar, well-defined, heterogeneosuly hypoechoic lesion, about 3,8 cm wide, with a striped appearance (arrows) and a thin hyperechoic capsule (arrowhead) is seen in the subcutaneous tissue. The lesion was grade 0 on CDUS.

ABSCESS (11)

Eight (72,7%) abscesses had heterogeneous echotexture. The longest diameter (size) ranged from 2,3 to 4,5 cm (mean, 3,3). 6 (54,5%) were hypoechoic, 5 (45,5%) isoechoic. The margins were ill-defined in 8 (72,7%). Shapes were irregular in 6 (54,5%) and oval in 5 (45,5%). On CDUS, 6 (54,5%) were classified as grade 0; 4 (36,4%) were classified as grade 1 (with capsular flow).

A spindle-shaped hyperechoic grass awn was identified within all abscesses (100%) (Fig. 26). Acoustic shadowing was associated with the grass awn in 8 (72,7%) cases.

Four (36,4%) abscesses were located in the extremities and 4 (36,4%) along the chest wall.

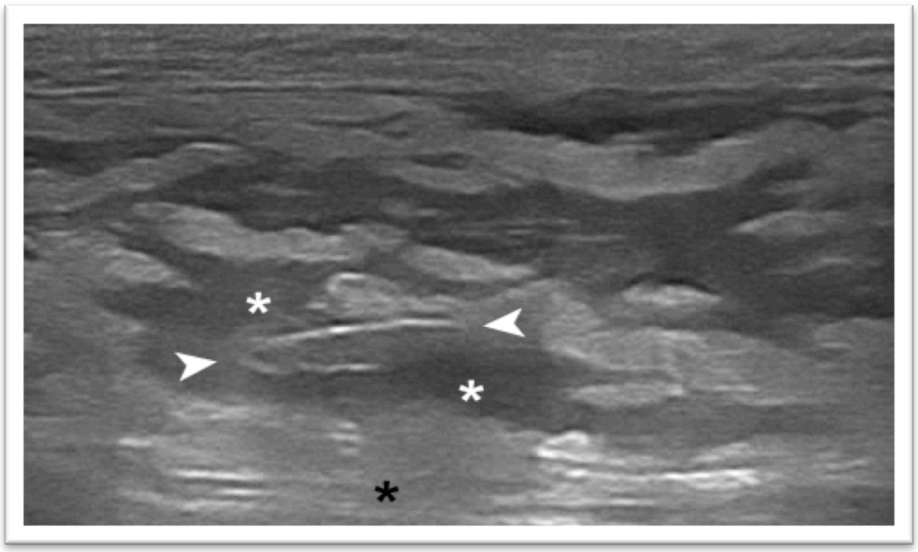

**Fig. 26. Dog, case 86**. Ultrasonographic image of a foreign body abscess of the neck region in a 1-year-old, castrated male, English Bulldog. An ovoid, ill-defined, heterogeneosuly hypoechoic lesion, about 4 cm wide, is seen in the subcutaneous tissue. A double, spindle shape echogenic interface (arrowheads), provided of mild acoustic shadowing (black asterisk), and surrounded by a hypoechoic halo (white asterisk), is observed in the middle of the abscess. The lesion was grade 0 on CDUS. A grass awn foreign body was removed.

GRANULOMA (4)

In this series granulomas were classified as: injection granuloma (n.2), infectious granuloma (n.1) and lick granuloma (n.1).

All 4 (100%) granulomas were oval in shape. Margins were well-defined in 2 (50%). The longest diameter (size) ranged from 1,7 to 3,9 cm (mean, 2,9). Three (75%) granulomas showed heterogeneous hypoechogenicity, with a "cobblestone" pattern most consistent with subcutaneous inflammation/edema (Fig. 27,28). On CDUS, 2 (50%) granulomas were classified as grade 0, 1 (25%) as grade 1 and 1 (25%) as grade 3. Three (75%) granulomas were identified along the dorsum.

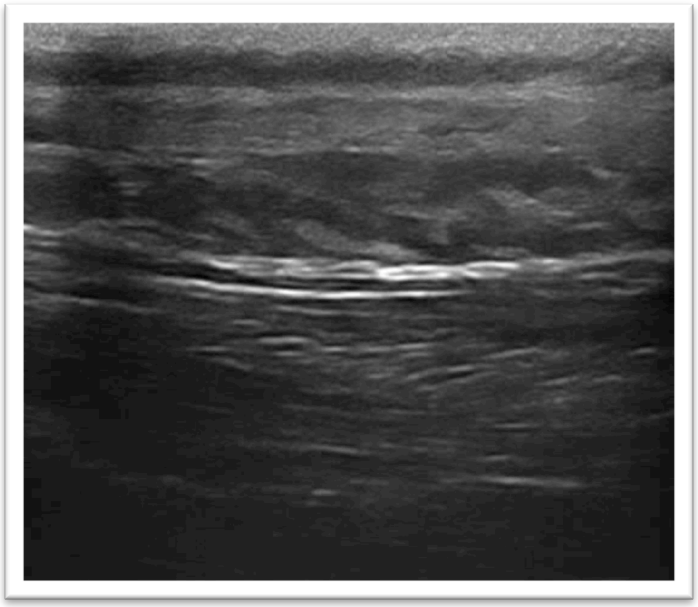

**Fig. 27. Dog, case 94**. Ultrasonographic image of a injection granuloma following antibiotic treatment in the interscapolar region of a 1-year-old, entire female, Labrador Retriever. An ovalar lesion, about 3 cm wide, is seen in the subcutaneous tissue. The lesion is heterogeneously hypoechoic, with fusiform hypoechoic areas dispersed randomly in a hyperechoic background (fat and connective tissue), resembling a "cobblestone" appearance.

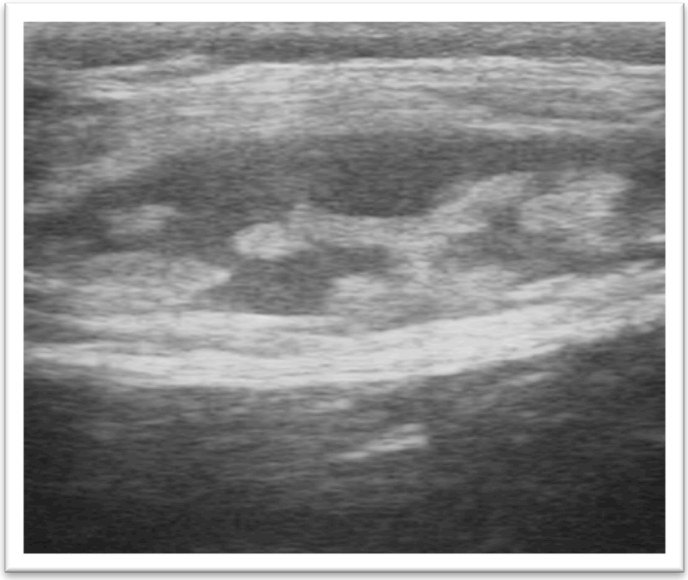

**Fig. 28. Dog, case 92.** Ultrasonographic image of a *Leishmania* granuloma in a 2 year-old, spayed female, Cane Corso. An ovalar, well-defined lesion, about 3 cm wide, is seen in the subcutaneous tissue of the dorsum. Interspersed hypoechoic and hyperechoic strands, resembling a "cobblestone" appearance, are seen within the lesion.

PYODERMA (2)

All of the cases of pyoderma were oval in shape, heterogeneously hyperechoic and with irregular margins. CDUS showed grade 3 for both lesions.

A peculiar pattern of hyperechoic stripes within hypoechoic areas was seen in both cases (Fig. 29,30) and considered most consistent with remnants of hair follicle within pustular lesions, as demonstrated on histological exam.

Both lesions (100%) were identified in the hindlimbs.

**Fig. 29. Dog, case 96**. Grayscale and CDUS of pyodermitis of the hindlimb in a 5-year-old, entire male, cross-breed dog. A 2,8 cm wide, heterogeneously hyperechoic lesion, with hypoechoic area (asterisks) and hyperechoic stripes (arrowhead) within is seen. CDUS was grade 3. The hypoechoic areas are most consistent with fluid collection, while the hyperechoic lines could correspond to hair tract fragments within the collection. Histology confirmed the presence of neutrophilic, pustular lesion associated with remains of hair follicles (furunculosis).

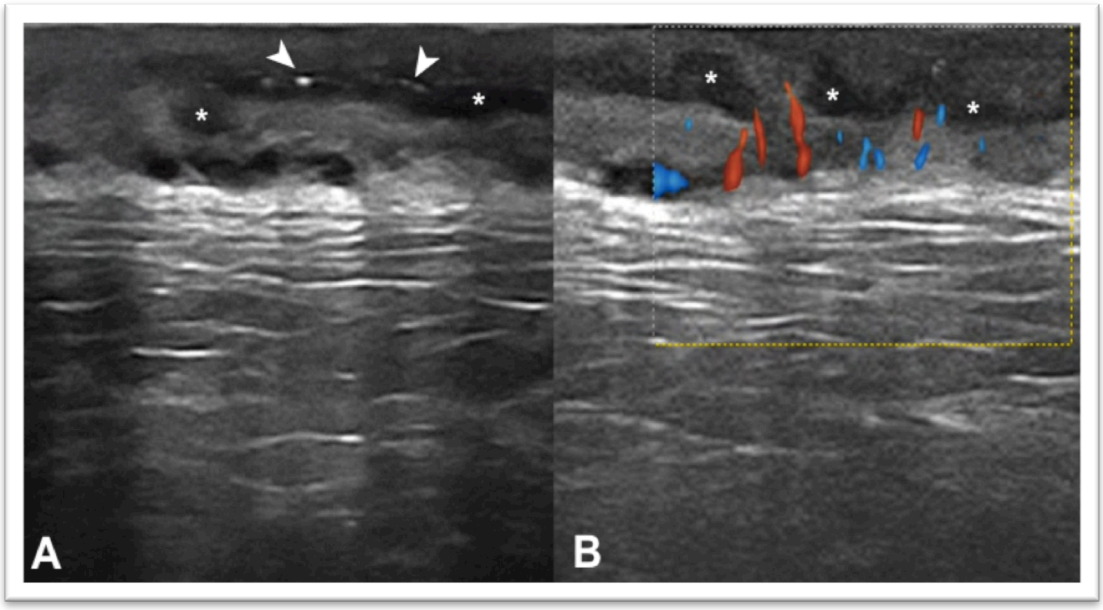


**Fig. 30. Dog, case 95**. (A) Grayscale US of pyodermitis of the hindlimb in a 7-year-old, entire male, German Sheperd dog. A 2,8 cm wide, heterogeneously hyperechoic lesion, with hypoechoic areas (asterisks) and hyperechoic stripes within (arrowheads) is seen. The hypoechoic areas are most consistent with fluid collection, while the hyperechoic lines could correspond to hair tract fragments within the collection. (B) CDUS shows grade 3 vascularity.

FOLLICULAR NEOPLASIA (3)

All follicular neoplasia (100%) were oval in shape. Two of them (66,7%) had well-defined margins. 2 (66,7%) were hypoechoic and 2 (66,7%) were heterogeneous in echotexture. CDUS were grade 0, 1 and 3. Two follicular neoplasia (66,7%) lesions were identified along the dorsum.

CUTANEOUS HISTIOCYTOMA (3)

Cutaneous histiocytomas (CHs) were all (100%) oval in shape, well-defined and homogeneously isoechoic (Fig. 31). The longest diameter (size) ranged from 0,8 to 1,5 cm (mean, 1,16 cm). They all were grade 1 on CDUS. 2 (66,7%) lesions were located in the extremities.

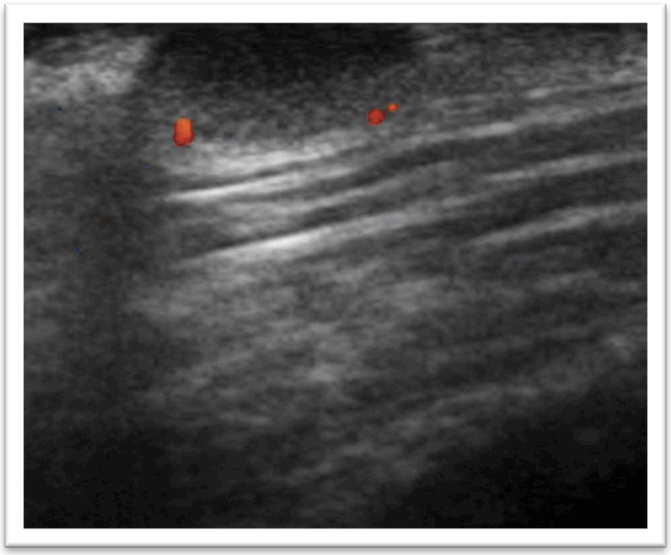

**Fig. 31. Dog, case 22**. Ultrasonographic image of a cutaneous histiocytoma of the hind limb in a 7-month cross-breed male dog. An ovalar, well-defined, isoechoic lesion, about 1,2 cm wide, with scant (capsular) vascular flow is seen. CDUS was grade 1.

## MALIGNANT LESIONS

METASTASES (7)

Distant metastatic nodules (METs) were classified as derived from breast carcinoma (2 cases), splenic HSA (1 case), laryngeal chondrosarcoma (1 case), and cutaneous MCT (1 case). Two cases (1 schwannoma and 1 sarcoma) were local recurrences in the primary tumor scar.

All 7 (100%) METs were homogeneously hypoechoic and polycyclic in shape (Fig. 32, 33). The longest diameter (size) ranged from 0,9 to 2,6 cm (mean, 1,78 cm). 5 (71,4%) had well-defined

margins. 5 (71,4%) had posterior acoustic shadowing. 6 lesions (85,7%) were graded 3 on CDUS.

4 METs (57,1%) occurred in the extremities.

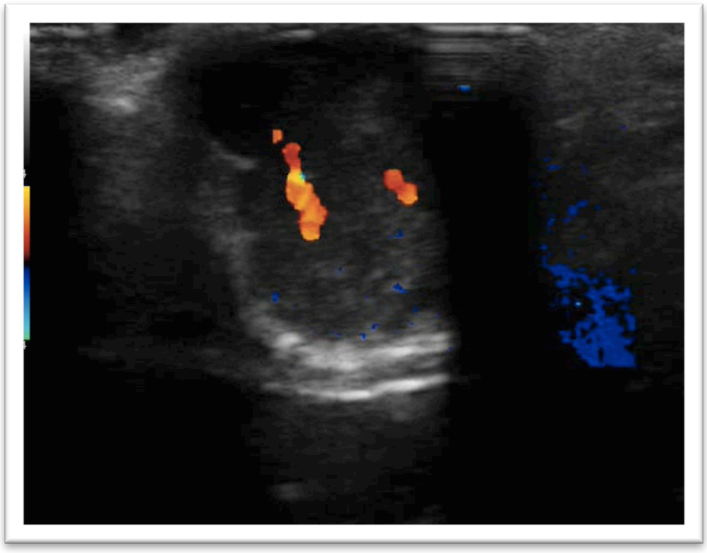

**Fig. 32. Dog, case 15**. A subcutaneous homogeneosuly hypoechoic nodule, about 2,6 cm wide, with polycyclic shape at the level of the hindlimb in a 13-year-old, entire male, cross-breed dog with previously diagnosed splenic HSA. CDUS was graded as 3. Hilar and peripheral flow is shown.

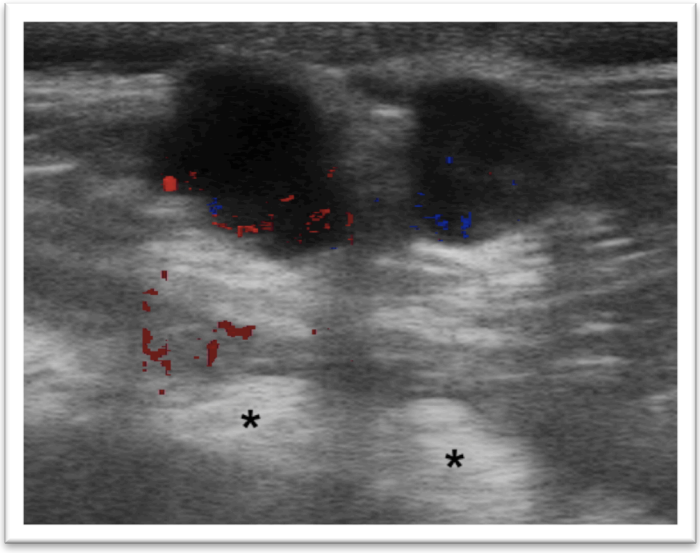

**Fig. 33. Dog, case 17.** Two homogeneously hypoechoic, about 1,5 cm wide, polycyclic in shape, nodules localized in the subcutaneous fat of the inguinal region in a 12-year-old entire female Golden Retriever with previously diagnosed schwannoma. Color Doppler imaging showed hypervascularity (grade 3) with peripheral and hilar vessels. Posterior enhancement is appreciated (asterisks).

HEMANGIOPERICYTOMA (5)

Hemangiopericytomas (HPCs) were all oval in shape, heterogeneously hypoechoic (Fig. 34) and with ill-defined margins. The longest diameter (size) ranged from 1,9 to 3,8 cm (mean, 2,86). 4 (80%) lesions were grade 3 on CDUS. All of them (100%) were located in the extremities.

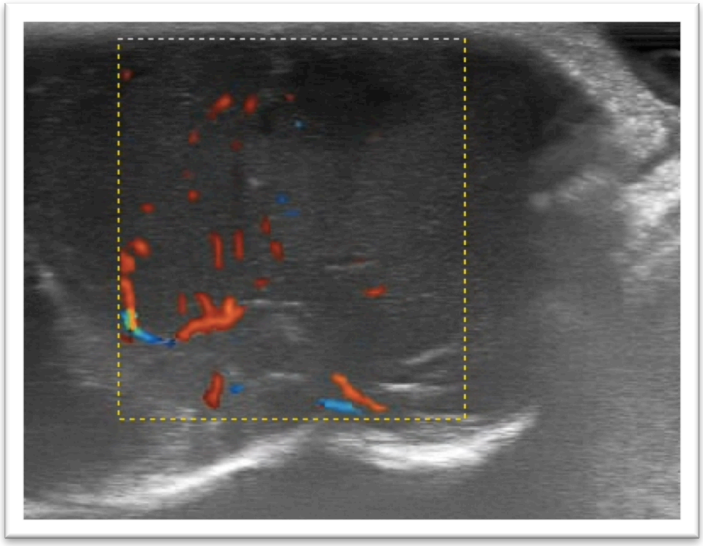

**Fig. 34. Dog, case 29**. Grayscale and Color Doppler ultrasonographic image of a hemangiopericytoma of the front limb in a 15-year-old, spayed female, cross-breed dog. The lesion is oval, with ill-defined margins, heterogeneously hypoechoic, about 3,8 cm wide. High vascular flow is seen (grade 3 on CDUS).

MAST CELL TUMOR (38)

Twenty-seven (71%) mast cell tumors (MCTs) had well-defined margins. Twenty (52%) MCTs were spear-shaped (elongated shape with pointed edges) (Fig. 35, 36), 15 (39,5%) were oval (Fig. 37), 3 (7,9%) were rounded. The longest diameter (size) ranged from 1,1 to 5,3 cm (mean, 2,66). 22 (57,9%) MCTs were isoechoic, 15 (39,5%) hypoechoic, 1 (2,6%) hyperechoic. 20 (52,6%) had homogeneous echotexture (Fig. 35,36,37). 4 (10,5%) lesions showed posterior acoustic enhancement. 17 (44,7%) lesions were graded 1 on CDUS. 6 (15,8%) were graded 2, 10 (26,3%)

were graded 3 and 5 (13,2%) were graded 0.

Of the 17 lesions with grade 1 on CDUS, 16 showed a capsular flow and displayed a main vascular pedicle entering the capsule in the deeper part of the lesion (Fig. 36, 37).

Twenty-four (63,2%) lesions were located in the extremities.

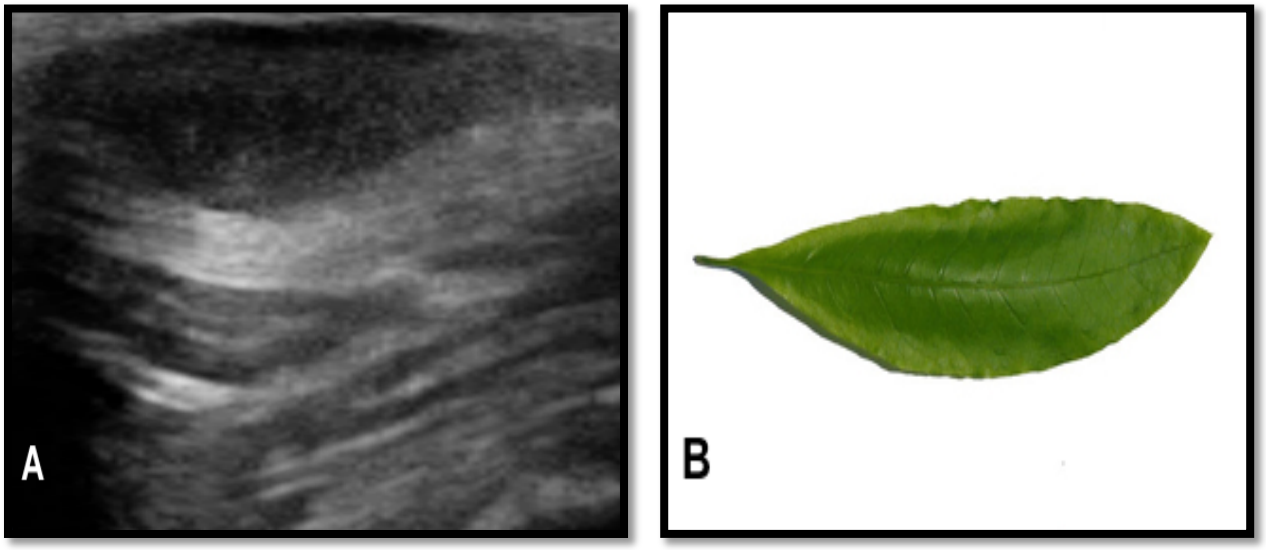


**Fig. 35. Dog, case 34**. (A) Grayscale ultrasonographic image of a cutaneous MCT of the chest wall in a 5-year-old, entire male, cross-breed dog. A spear-shaped, well-defined, homogeneously hypoechoic lesion, about 1,9 cm wide, and with no vascularization is seen. (B) Image illustrating the spear-shaped appearance of a leaf.

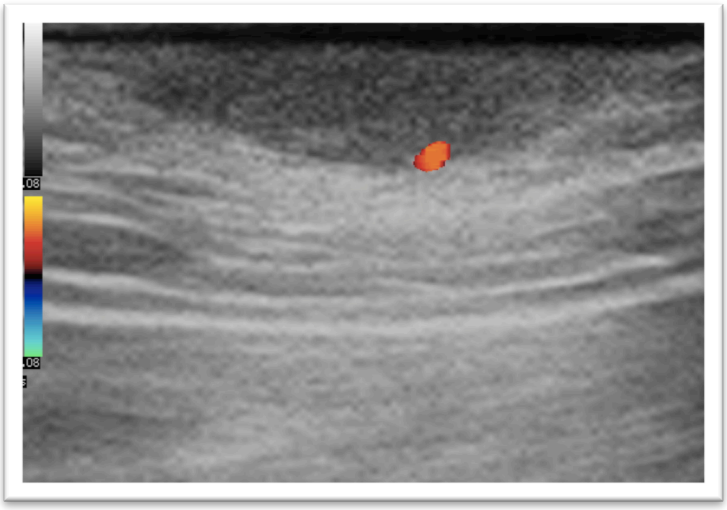

**Fig. 36. Dog, case 64**. (A) Grayscale and CDUS image of a cutaneous MCT in the axillary region in a 8-year-old, spayed female, crossbreed dog. A spear-shaped, well-defined, homogeneously isoechoic lesion, about 2,2 cm wide. A capsular vascularization with a main vascular pedicle is seen. CDUS was grade 1.

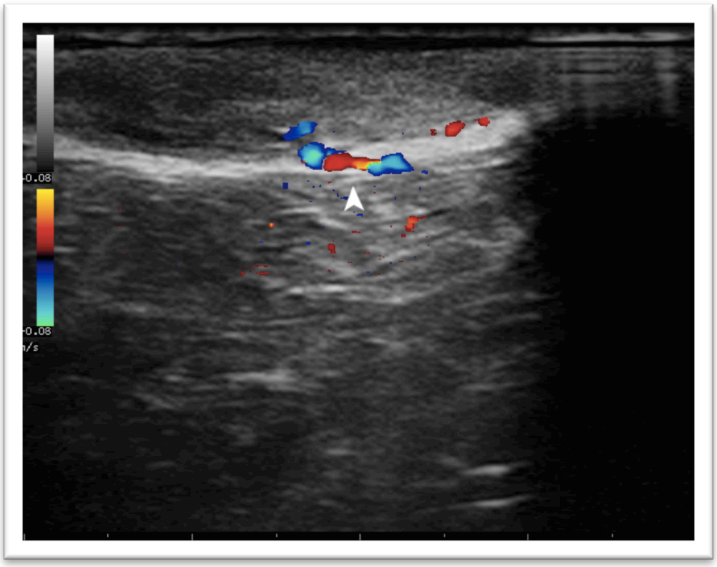

**Fig. 37. Dog, case 46**. (A) Grayscale and CDUS ultrasonographic image of a cutaneous MCT of the hind limb in a 5-year-old, entire male, cross-breed dog. A oval, well-defined, fairly homogeneously isoechoic lesion, about 2,8 cm wide, with capsular vascularization is seen. A main vascular pedicle entering the capsule is appreciated (white arrowhead). CDUS was grade 1.

APOCRINE SWEAT GLAND CARCINOMA (1)

The apocrine sweat gland carcinoma was polycyclic in shape, with ill-defined margins, homogeneously hypoechoic and associated with posterior acoustic enhancement. On CDUS, the lesion was grade 2 (capsular flow).

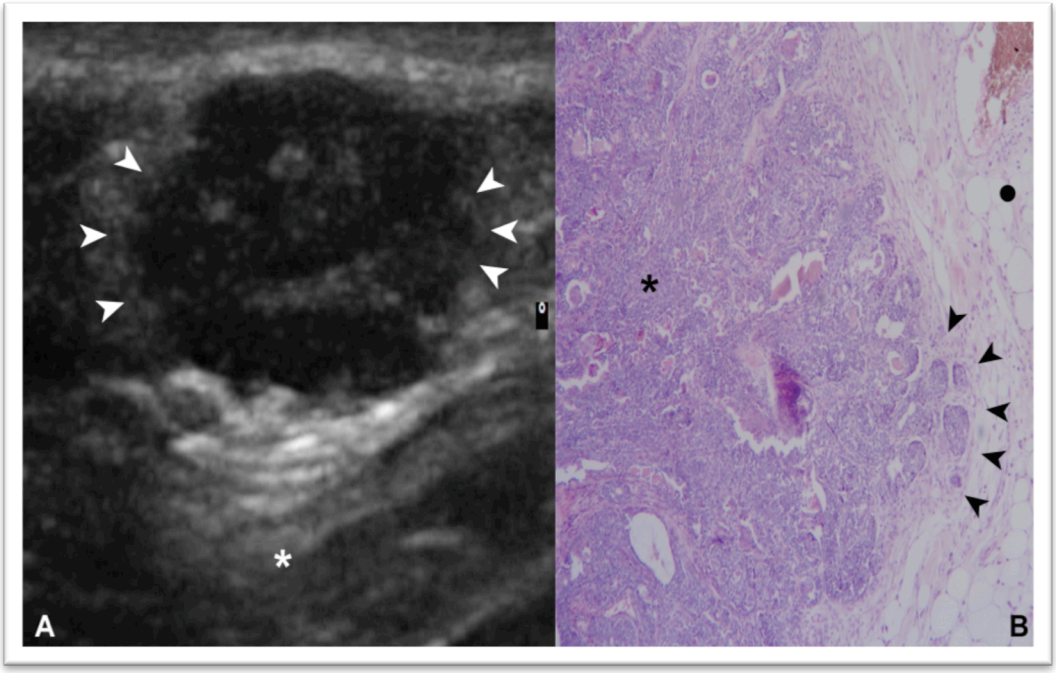


**Fig. 38. Dog, case 107**. (A) Grayscale US of apocrine sweat gland carcinoma of the dorsum in a 3-year-old, entire male, Labrador Retriever. A 1,2 cm wide homogeneously hypoechoic lesion, with polycyclic shape (white arrowheads) and ill-defined margins is shown. Acoustic shadowing is appreciated (white asterisk). (B) Histologic section of the lesion showing proliferation of neoplastic cells (black asterisk). Along the margins of the lesion, infiltration of neoplastic cells (arrowheads) into the adipous tissue (black circle) is seen. Infiltrating margin on histology correlates with the polycyclic shape observed in the ultrasonographic image (figure A).

For other single lesions type, results of the ultrasonographic examination are provided in Table 3.

## *Statistical results*

Lesion size, border, echogenicity were not significant indicators for differentiating benign from malignant lesions ($P > 0,05$). On the other hand, shape, echotexture, acoustic shadowing and CDUS seemed to be significant indicators for distinguishing benign from malignant lesions ($P < 0,05$).

Spear-shape and polycyclic shape were features indicative of malignant lesions. In particular, spear-shape was 100% sensitive and 100% specific for MCTs. A polycyclic shape was a sign 100% sensitive and 78 % specific for METs.

Furthermore, high grades on CDUS (2-3) were statistically significant associated to malignancy.

On the other hand, heterogenicity and acoustic shadowing were significant indicators of benign lesions.

A significant Pearson correlation coefficient was found between major and minor diameter of the lesions ($r = 0,758$; $P < 0,001$).

Finally, there was no significant difference in the sex distribution between the patients presenting with benign or malignant lesions ($P > 0,05$).

# DISCUSSION

This study evaluates the usefulness of HFUS in the clinical assessment of many skin diseases of dogs, including neoplasms, inflammatory lesions and other conditions.

Because of the mix of tumor types investigated in this study, and the fact that some tumors are diagnosed using cytology and others by histopathology, it is difficult to draw specific conclusions on different histological type of tumors. Specific tumor types, however, are mentioned separately when relevant.

The smallest lesion examined was 0,4 x 0,2 cm, which show the possibility of investigating even small nodules with high-frequency probes.

***Benign lesions***

The study shows that the typical pattern of unruptured ICs is similar to what reported in human literature and include a heterogeneous hypoechogenicity, solid composition, a well-defined margin, oval shape, posterior enhancement, and a grade 0 on CDUS (Kim *et al*, 2011; Lee *et al*, 2001). About 71,4% of subjects with ICs in this series had internal hyperechoic bright striations disseminated over the lesion, which were probably related to the presence of scattered keratin debris.

Furthermore, specific patterns classified as “onion ring”, “tram track” and “pseudotestis” were observed in association with three intact ICs in our series, similar to that which has been reported in human literature (Huang *et al*, 2011; Rahul *et al*, 2015).

In the only case of ruptured IC, ill-defined margins and mild peripheral vascularization were appreciated (grade 1 CDUS). Similarly, in human medicine, ruptured ICs can result in internal vascularity (70%) secondary to the local irritant effect of leaked keratin. Poorly defined boundaries

are usually present in these cases (Yuan *et al,* 2012).

HFUS may represent a critical point in the evaluation of ICs, as these lesions, on palpation, can mimic other subcutaneous cystic masses or solid tumours. Furthermore, cytological exam can provide a presumptive diagnosis of ICs, but it is not sufficient to reliably rule out neoplasia (Hong *et al,* 2006). Within this context, the use of HFUS may provide further information and help in ruling out a neoplastic disease.

This study confirms previous reports of the ultrasonographic characteristics of lipomas; namely thin, parallel, hyperechoic lines compared with the surrounding tissue (Nyman *et al*, 2006; Volta *et al*, 2006; Loh *et al*, 2009).

Foreign body abscesses in our series were avascular, heterogeneously hypoechoic or isoechoic lesions, irregularly-shaped, with well or ill-defined margins, similar to previous human and veterinary studies (Diaz, 2014; Zwingerberger *et al*, 2015). A potential explanation emerges from the tendency of abscesses to change in sonographic appearance over time. The different echogenicity of these lesions could be related to the different maturity and content of the abscess cavity (Adhikari and Blaivas, 2012).

Grass awns were identified within all the 11 abscesses and appeared as a double/triple spindle shape echogenic interface. Acoustic shadowing associated with the grass awn was identified in the 72,7 % of the subjects. Ultrasonographic appearance of grass awns in this series was consistent with previous reports (Gnudi *et al*, 2005).

As a histological exam was not performed on this category of lesions, we could not completely excluded that an underlying granuloma was concurrently present. Both granulomas and abscesses are reported to be common complications following foreign bodies penetration and can concurrently occurr (Della Santa *et al*, 2008). In our series, we preferred to categorize the lesions as "foreign body abscess" because the clinical picture and the presence of fistula tracts were

considered more consistent with an abscess formation.

3 (75%) granulomatous lesions in our series (2 injection site and 1 infectious granuloma) showed a "cobblestone" appearance on US, that is fusiform anechoic to hypoechoic areas (fluid) dispersed randomly in a hyperechoic background (fat and connective tissue). The "cobblestone" appearance represents a non-specific ultrasonographic pattern, usually related to subcutaneous edema or panniculitis (Chau and Griffith, 2005).

Actually, panniculitis has been reported to be a possible histological reaction pattern of granuloma (injection site or infectious) in both human and dogs (Chong *et al*, 2006; O'Kell *et al*, 2010; Neuber, 2011).

When a cobblestone pattern associated with a nodule/mass is seen, the possibility of an underlying granulomatous condition (infectious/non-infectious) should be considered in the differential diagnosis.

A peculiar pattern of hyperechoic stripes within hypoechoic areas, representing remnants of hair follicle within pustular lesions, was seen in both cases of pyoderma in our series.

This pattern partially resembled the "foreign body" pattern, consisting of a hyperechoic linear structure (foreign body) surrounded by a hypoechoic halo (hematoma, edema, fluid) (Shiels *et al*, 1990).

Actually, during pyoderma, hair follicle may rupture with subsequent liberation of keratin, which act as a foreign body within the dermis, perpetuating the cycle of inflammation (Lewis, 2010). The severe grade of inflammation which characterizes these lesions resulted in a high grade (3) of vascularization on CDUS.

We may assume that, on US, not all the hyperechoic linear structures surrounded a by a hypoechoic halo represent "true" foreign bodies. Hair follicle inflammation secondary to pyoderma may mimic

the presence of small foreign bodies within the skin. Clinical findings and follow-up US may help to confirm the presence of "true" foreign bodies in equivocal cases.

Although artifacts are usually considered detrimental to the quality of images, acoustic shadowing and enhancement may have diagnostic value by revealing some additional characteristics of the tissues (Loh *et al*, 2009).

In our series, all the CHs were oval, well-defined, homogeneous and isoechoic lesions, with grade 1 on CDUS. In a previous study, 6 benign CHs were reported to be homogenously isoechoic lesions with the surrounding tissue, but unfortunately no clear information about margins and vascularization was provided in that paper (Nyman *et al*, 2006).

Although CHs are usually benign lesions which undergo spontaneous regression within few months, surgical resection and histopathology are recommended for lesions which do not regress over long periods (Fulmer and Mauldin, 2007). Within this context, exploring possible ultrasonographic patterns of CHs could be helpful in order to promptly identify suspicious or atypical lesions.

***Malignant lesions***

This study showed that the typical pattern of superficial soft-tissue METs was homogeneous hypoechogenicity, polycyclic shape, well-defined margins, acoustic enhancement and high grade of vascularization (grade 3 on CDUS).

A polycyclic shape and hypervascularity were considered the most indicative signs of skin metastasis in a human study, with a high specificity for METs (100%) (Giovagnorio *et al*, 2003).

In our study, a polycyclic shape was observed in all cases of METs and in 2 cases of malignant neoplasia (1 cutaneous melanoma and 1 apocrine sweat gland carcinoma). Accordingly to these results, we can assume that a polycyclic shape was a sign 100% sensitive and 100% specific for

malignancy. On the other hand, a polycyclic shape was a sign 100% sensitive and 78 % specific for METs.

A polycyclic shape was related to signs of infiltration of the surrounding tissues on histology; therefore, irregular borders should be considered expressions of local aggressiveness.

The markedly hypoechoic appearance, homogenicity and increased acoustic through-transmission shown by METs are likely related to the their tendency to be highly cellular and therefore to have fewer acoustic interfaces than the surrounding soft tissues (Nazarian *et al*, 1998).

The importance of exploring ultrasonographic patterns of superficial soft-tissue METs is related to the prognostic information for the patient. METs to superficial soft-tissues seem to be a late manifestation of advanced disease, in people as well as in animals (Tunio *et al*, 2013; Vignoli *et al*, 2013). This was further confirmed by our study, as METs to the superficial soft-tissues were associated with an end-stage disease and with the presence of METs in other body sites.

The most indicative features of MCTs in our study were a spear-shape and the presence of a capsular vascularization (with a main pedicle entering the capsule) (P = 0,001).

In the veterinary literature, ultrasonographic features of cutaneous MCTs have been described and included a homogeneous echotexture, well-defined margins and the presence of subcapsular vessels (Loh *et al*, 2009). In that paper, the authors subjectively discriminated among subcapsular, capsular and extracapsular (in close proximity to the outside of the tumor) vessels.

We preferred to categorize vascularization in MCTs as hilar, peripheral and capsular, because, to our opinion, precise discrimination between capsular and subcapsular vessels can be challenging and misleading.

A spear-shape was a sign observed only in MCTs in our study and therefore should be considered specific (100%), although lacking in sensitivity (52%).

Early diagnosis of mast cell disease is important, because there are a number of precautions that may be taken if the diagnosis is known preoperatively (Rogers, 2010). Specifically, if MCT is known or suspected, premedication with $H_1$ and $H_2$ receptor blockers should be given in order to minimize degranulation post-aspirate, potential swelling and local haemorrhage (Rogers, 2010).

Within this context, HFUS could be a useful exam to include in the initial diagnostic work-up of cutaneous MCTs, in association with clinical examination.

HPCs in our series were oval shaped, ill-defined, heterogeneously hypoechoic and hypervascular lesions. In a previous paper, ultrasonographic features of soft tissue sarcoma have been described, although no distinction between histological types of sarcoma was provided (Loh *et al*, 2009).

In that paper, no specific ultrasonographic features of soft tissue sarcomas were found; however, there was a trend for soft tissue sarcomas to have a larger size than the other groups of tumors, partly because of their highly invasive nature. This trend was also seen in our series, as HPC showed the highest mean tumor size among neoplastic lesions. However, as already reported, size was not a statistically significant parameter for distinguishing between benign and malignant lesions in our study.

***Benign vs. malignant lesions***

Acoustic enhancement arises posterior to any lesion that attenuates sound less than the surrounding tissue; the intensity of the transmitted ultrasound beam is relatively preserved distal to the lesion (Bushberg *et al*, 2002). Posterior acoustic enhancement is most commonly discussed in the context of cystic lesions, although solid masses may also be associated with increased through transmission (Hertzberg and Middleton, 2016).

In our series, both ICs and METs had a significantly higher frequency of acoustic shadowing than other lesion type ($P < 0,05$). However, it remains clear that this artifact is not a good indicator for differentiating benign from malignant lesion ($P > 0,05$).

Distal shadowing is another type of ultrasonographic artifact seen when a highly reflective structure attenuates ultrasound propagation (Nyman *et al*, 2006). In our series, distal shadowing was significantly associated with benign lesions, in particular with foreign body abscesses (P = 0,03). However, this result should be interpreted with caution, as the distal shadowing was related most probably to the presence of the foreign body and not to the abscess itself.

Echotexture was a good indicator for differentiating benign from malignant lesions in this study (P = 0,001). Actually, heterogeneous echotexture was a significant feature indicative of a benign lesion, such as infundibular cysts, lipomas, abscesses and granulomas.

Interestingly, in a human study, the only specific ultrasonographic finding of benignity for cutaneous lesions, such as granulomas and sebaceous cysts, was the presence of intralesional calcifications and strong echoes, which gave rise to a heterogeneous echotexture (Giovagnorio *et al*, 2003). This finding was considered a typical expression of the histologic nature of those nodules because granulomas may develop around intensely echoic foreign bodies, and sebaceous cysts typically contain necrotic material, sebum, and degraded hair, which may produce strong internal echoes and eventually calcify (Rook *et al*, 1968). Although, theoretically, cutaneous metastases from certain classes of tumors may calcify, analysis of the literature suggest that the presence of calcifications in the nodule is an almost sure expression of benignity in humans (Giovagnorio *et al*, 2003).

A similar mechanism may be hypothetized in our study for infundibular cysts, abscesses and granuloma, being the histopathological aspect comparable to what have been observed in human beings.

It deserves being mentioned that mammary nodules were not included in the study of Giovagnorio *et al*, similarly to our study. Micro and macrocalcifications represent quite a common finding in mammary neoplasia (benign and malignant) in both human and dogs (Mohammed *et al*, 2011).

A significant difference was found in our study between benign and malignant lesions with regard to the grade of vascularization on CDUS. A CDUS of 2-3 was highly associated with malignant lesions (P = 0,001).

This result resembles previous findings in both human and veterinary literature (Nyman *et al*, 2006; Catalano & Siani, 2007).

Malignant tumors are faster growing and therefore need a greater blood supply to support this rapid growth (Nyman *et al*, 2006). In malignant tumors, vascularization correlates with invasive potential (Gutberlet and Rudolph, 1994; Folkman, 1995) and seems to determine tumor progression. Furthermore, intratumoral microvessel density is well known to be a prognostic factor in several tumor types (Nyman *et al*, 2006).

About vessel distribution, hilar and capsular distribution were significant indicators of a malignant lesions (P < 0,05). Conversely, periferal flow was not a good parameter for distinguishing between benign and malignant lesions (P > 0,05).

Our study had a number of limitations.

First of all, not all the patients had pathological diagnosis. Some cases with higher benign probability were confirmed by typical imaging findings and comprehensive diagnosis in follow-up.

Secondly, we reviewed the images by consensus, without any calculation of interobserver agreement.

Additionally, our description of the lesions and categorization of the degree of Doppler vascularization was somewhat subjective. Differentiation between homogeneous and heterogeneous lesion was simplified, as we did not consider fine and coarse architecture. Also, among hypoechoic lesions, some were markedly hypoechoic and other non-markedly hypoechoic, but we decided to consider all these togheter in order to simplify the report.

# CONCLUSIONS

Superficial soft tissue lesions, both inflammatory and neoplastic, are common in dogs.

In veterinary medicine, HFUS has traditionally had a limited role in evaluating soft-tissue lesions.

Although some paper exist demonstrating the feasibility of US for the evaluation of superficial soft tissue lesions, HFUS is not routinely applied for evaluation of this category.

This paper shows that the resolution of current sonography in veterinary medicine may allow the identification of patterns comparable to those observed in humans, paving the way for the use of HFUS in the diagnosis of skin diseases in small animals.

In conclusion:

1) A spear shape and a capsular vascularizarization are characteristic features of MCTs;

2) A polycyclic shape is characteristic of malignant lesions and, in particular, of METs;

3) Echotexture, shape, CDUS, are the most important ultrasonographic classification criteria when evaluating superficial soft-tissue lesions.

High-frequency ultrasonography may be very useful in the assessment of superficial soft tissue lesions.

Otherwise, US is not intended to replace histology but perhaps can provide a missing link between the clinical evaluation, and the later, biopsy and treatments.

Further studies are required in veterinary medicine to investigate possible sonographic patterns of superficial soft-tissue lesions, with the final aim to reduce invasive procedures like fine needle aspirations and biopsies. Also, future studies using a larger sample size may yield statistically significant results, including differentiation of tumor grade.

In the near future, high-frequency ultrasonographic exam could play a complementary role to physical examination in the assessment, diagnosis and management of skin lesions in dogs.

# REFERENCES


Abramo F, Albanese F, Masserdotti C. Malattie dermatologiche. 1st ed. UTET scienze mediche, 2009.

Adhikari S and Blaivas M. Sonography first for subcutaneous abscess and cellulitis evaluation. *J Ultrasound* Med 2012;31:1509-1512.

Adhikari RC, Shrestha KB, Sayami G. Granulomatous inflammation: A histopathological study. *Journal of Pathology of Nepal* 2013; 3:464 – 468.

Alexander H and Miller DL. Determining skin thickness with pulsed ultrasound. *J Invest Dermatol* 1979;72:179.

Altmeyer P, El-Gammal S, Hoffman K. Berlin. *Ultrasound in Dermatology*. Springer, 1992.

Ando A, Hatori M, Hagiwara Y, Isefuku S Itoi E. Imaging features of foreign body granuloma in the lower extremities mimicking a soft tissue neoplasm. *Upsala Journal of Medical Sciences* 2009; 114:46-51.

Armbrust LJ, Biller D, Radlinsky MG, Hoskinson JJ. Ultrasonographic diagnosis of foreign bodies associated with chronic draining tracts and abscesses in dogs. *Vet Radiol Ultrasound* 2003;44:66–70.

Atlee BA, DeBoer DJ, Ihrke PJ *et al*. Nodular dermatofibrosis in German Sheperd dogs as a marker for renal cystadenocarcinoma. *J Am Anim Hosp Assoc* 1991;27:481-487.

Badea R, Crisan M, Lupsor M, Fodor L. Diagnosis and characterization of cutaneous tumor using combined ultrasonographic procedures (conventional and high resolution ultrasonography). *Med Ultrason* 2010;12:317-322.

Bigham AS and Nourani H. Subcutaneous cellulitis of the thigh due to grass awn migration in a German Sheperd dog. *Comp Clin Pathol* 2009;18:197.

Botchu R, Khan A, Bhatt R. Pictorial essay: USG of lumps and bumps of the foot and ankle. *Indian Journal of Radiology and Imaging* 2010;20:105-108.

Breslow A. Thickness, cross-sectional areas and depth of invasion in the prognosis of cutanoeus melanoma. *Ann Surg* 1970;172:902-908.

Bushberg J, Seibert J, Leidholdt E, *et al*. *The Essential Physics of Medical Imaging*. 2nd ed. Philadelphia, PA: Lippincott Williams & Wilkins;2002.

Cammarota T, Pinto F, Magliaro A, Sarno A. Current uses of diagnostic high-frequency US in dermatology. Eur J Radiol. 1998;27:215-223.

Cardinal E, Bureau NJ, Aubin B, *et al*. Role of ultrasound in musculoskeletal infections. *Radiol Clin North Am* 2001;39:191–201.

Catalano O, Siani A. (eds) Ecografia e oncologia. In: Ecografia in oncologia. Testo Atlante di Ultrasonologia. 1st edn. Springer. 2007:1-25.

Catalano O, Siani A. Cutaneous melanoma: role of ultrasound in the assessment of locoregional spread. *Curr Probl Diagn Radiol* 2010;39:30-36.

Chami L, Lassau N, Chebil M, *et al*. Imaging of melanoma: usefulness of ultrasonography before and after contrast injection for diagnosis and early evaluation of treatment. *Clin Cosmet Investig Dermatol* 2011;4:1–6.

Chau CLF, Griffith JF. Pictorial review Musculoskeletal infections: ultrasound appearances. *Clinical Radiology* 2005;60:149–159.

Chen M, Sarma D. Wooden splinter dermatitis. *Internet Journal of Dermatology* 2007;5:1-3.

Chiou HJ, Chou YH, Chiou SY, *et al*. High-resolution Ultrasonography in Superficial Soft Tissue Tumors. *J Med Ultrasound* 2007;15:152-174.

Chiou HJ, Chou YH, Chiu SY, *et al*. Differentiation of benign and malignant superficial soft-tissue masses using Grayscale and Color doppler ultrasonography. *J Chin Med Assoc* 2009;72:307-315.

Chong H, Brady K, Metze D, *et al*. Persistent nodules at injection sites (aluminium granuloma) - clinicopathological study of 14 cases with a diverse range of histological reaction patterns. *Histopathology* 2006;48:182-188.

Cooley DM, Allen DK, Waters DJ, *et al*. Vascular neoplasms of dogs. *Kleintierpraxis* 1997;42:859–870.

Cooper RA, Ramamurthy L. Epidermal inclusion cyst in the male breast. *Can Assoc Radiol J* 1996; 47:92.

Crystal P, Shaco-Levy R. Concentric rings within a breast mass on sonography: lamellated keratin in an epidermal inclusion cyst. *AJR Am J Roentgenol* 2005;184:47-48.

De Rigal J, Escoffier C, Querleux B, *et al*. Assessment of aging of the human skin by in vivo ultrasonic imaging. *J Invest Dermatol* 1989;93:621–625.

Della Santa D, Rossi F, Carlucci F, *et al*. Ultrasound-guided retrieval of plant awns. *Vet Rad Ultrasound* 2008;49:484-486.

Diana A, Preziosi S, Guglielmini C, *et al*. High-frequency ultrasonography of the skin of clinically normal dogs. *AJVR* 2004;65:1625-1630.

Diana A, Guglielmini C, Fracassi F, *et al*. Use of high-frequency ultrasonography for evaluation of skin thickness in relation to hydration status and fluid distribution at various cutaneous sites in dogs. *AJVR* 2008;69:1148-1152.

Díaz CPG. Characterization of dermatological lesions by Ultrasound. *Rev Colomb Radiol* 2014; 25:4006-4014.

Dubois J, Patriquin HB, Garel L, *et al*. Soft-tissue hemangiomas in infants and children: diagnosis using Doppler sonography. *AJR Am J Roentgenol* 1998;171:247-252.

Fabbi M, Di Palma S, Manfredi S, *et al*. Imaging diagnosis- ultrasonographic appearance of skeletal muscle metastases in a dog with hemangiosarcoma. *Vet Radiol Ultrasound* 2016;Oct 4.doi: 10.1111/vru.12432.

Fayad L, Carrino J, Fishman L, *et al*. Musculoskeletal infection: role of CT in the emergency department. *Radiographics* 2007;27:1723-1736.

Fernandez-Flores A, Valerdiz S, Crespo LG, *et al*. Granulomatous response due to anabolic steroid injections. *Acta Dermatovenerol Croat* 2011;19:103-106.

Folkman J. Angiogenesis in cancer, vascular, rheumatoid and other disease. *Nat Med* 1995;1:27–31.

Fornage BD, Tassin GB. Sonographic appearances of superficial soft tissue lipomas. *J Clin Ultrasound* 1991;19:215-220.

Fornage BD, McGavran MH, Duvic M, *et al*. Imaging of the skin with 20-MHz US. *Radiology* 1993;189:69–76.

Fulmer AK, Mauldin GE. Canine histiocytic neoplasia: An overview. *Can Vet J* 2007;48:1041–1050.

Gilbert PA, Griffin CE, Walder EJ. Nodular dermatofibrosis and renal cystadenoma in a German Sheperd dog. *J Am Animal Hosp Ass* 1990;26:253-256.

Giovagnorio F, Valentini C, Paonessa A. High-resolution and color doppler sonography in the evaluation of skin metastases. *J Ultrasound Med* 2003;22:1017-1022.

Gniadecka M, Gniadecki R, Serup J, *et al*. Ultrasound structure and digital image analysis of the subepidermal low echogenic band in aged human skin: diurnal changes and interindividual variability. *J Invest Dermatol* 1994;102:362–365(a).

Gniadecka M, Serup J, Sondergaard J. Age-related diurnal changes of dermal oedema: evaluation by high-frequency ultrasound. *Br J Dermatol* 1994;131:849–855(b).

Gnudi G, Volta A, Bonazzi M, *et al*. Ultrasonographic features of grass awn migration in the dog. *Vet Radiol Ultrasound* 2005;46:423-426.

Goldschmidt MH, Shofer FS. *Skin tumours of the dog and cat*. Pergammon Press, Oxford, 1992; 271-291.

Gonzalez de Bulnes A, Garcia Fernandez P, Mayenco Aguirre AM, *et al*. Ultrasonographic imaging of canine mammary tumours. *Vet Rec* 1998;143:687–689.

Gross TL, Ihrkep J, Waloere J. (eds) Follicular tumors. In: *Veterinary Dermatopathology: A Macroscopic and Microscopic Evaluation of Canine and Feline Skin Disease*. C. V. Mosby-Yearbook. St Louis, 1992;351-373.

Gutberlet K, Rudolph R. Immunohistochemical identification of vessels in cancer cell invasion in canine mammary tumours. *Eur J Vet Pathol* 1994;1:11–14.

Hertzberg BS, Middleton WD (eds). Practical Physics. In: *Ultrasound: The requisites*, 3rd edn. Elsevier, Philadelphia, 2016;3-31.

Hillier A, Lloyd DH, Scott Weese J, *et al*. Guidelines for the diagnosis and antimicrobial therapy of canine superficial bacterial folliculitis. *Vet Derm* 2014; DOI: 10.1111/vde.12118.

Hong SH, Chung HW, Choi JY *et al*. MRI findings of subcutaneous epidermal cysts: emphasis on the presence of rupture. *AJR Am J Roentgenol* 2006;186:961-966.

Horton LK, Jacobson JA, Powell A, *et al*. Sonography and radiography of soft-tissue foreign bodies. *Am J Roentgenol* 2001;176:1155-1159.

Houston DM, Radostits OM, Mayhew IG. Clinical examination of the integumentary system. In: Radostis OM, Mayhew IG, Houston DM, eds. *Veterinary clinical examination and diagnosis*. 1st ed. London: WB Saunders Co, 2000;213–243.

Huang CC, Ko SF, Huang HY *et al*. Epidermal cysts in the superficial soft tissue: sonographic features with an emphasis on the pseudotestis pattern. *J Ultrasound Med* 2011;30:11-17.

Inampudi P, Jacobson JA, Fessell DP, *et al*. Soft-Tissue Lipomas: Accuracy of Sonography in Diagnosis with Pathologic Correlation. *Radiology* 2004;233:763-767.

Jacobson JA, Powell A, Craig JG, *et al*. Wooden foreign bodies in soft tissue: detection at US. *Radiology* 1998;206:45-48.

Joyce S, Rao Sripathi BH, Mampilly MO, *et al*. Foreign body granuloma. *J Maxillofac Oral Surg* 2014;13:351. doi:10.1007/s12663-010-0113-9.

Kahn CM, Line S. Skin disorders of dogs. In: *The Merck Manual for Pet Health.* 1st edn. NJ,USA:Merck & Co, Whitehouse station, 2007;238-283.

Kim HK, Kim SM, Lee SH *et al*. Subcutaneous epidermal inclusion cysts: ultrasound (US) and MR imaging findings. *Skeletal Radiol* 2011;40:1415-1419.

Kirkham N. Tumours and cysts of the epidermis. In: Elder D, eds. *Lever's Histopathology of the skin*. 8th edition. Philadelphia, PA: Lippincott-Raven, 1997;964-995.

Kleinerman R, Whang TB, Bard RL, *et al*. Ultrasound in dermatology: Principles and applications. *J Am Acad Dermatol* 2012;67:478-487.

Kransdorf MJ, Murphey MD. Radiologic evaluation of soft-tissue masses: a current perspective. *AJR Am J Roentgenol* 2000;175:575–587.

Lassau N, Lamuraglia M, Koscielny S, *et al*. Prognostic value of angiogenesis evaluated with high-frequency and colour Doppler sonography for preoperative assessment of primary cutaneous melanomas: Correlation with recurrence after a 5-year follow-up period. *Cancer Imaging* 2006;25:24-29.

Lee HS, Joo KB, Song HT *et al*. Relationship between sonographic and pathologic findings in epidermal inclusion cysts. *J Clin Ultrasound* 2001;29:374-383.

Lee Gross T, Ihrke PJ, Walder EJ, *et al*. (eds) *Skin Diseases of the Dog and Cat: Clinical and Histopathologic Diagnosis.* 2nd edn. Wiley-Blackwell. 2005:604-640.

Lewis DT. Dermatological disorders. In Schaer M, editor: *Clinical medicine of the dog and cat*. 2nd edn. Manson Publishing. 2010:9-48.

Liptak JM, Forrest LJ: Soft tissue sarcomas. In Withrow SJ, Vail DM, editors: *Small animal clinical oncology*. 4th edn. WB Saunders, Philadelphia, 2007:425–454.

Lium B, Moe L. Hereditary multifocal renal cystadenocarcinomas and nodular dermatofibrosis in the German Sheperd dog: macroscopic and histologic changes. *Vet Pathol* 1985;22:447-455.

Lloyd DH, Garthwaite G. Epidermal structure and surface topography of canine skin. *Res Vet Sci* 1982;33:99-104.

Lloyd D.H., Garthwaite G. Epidermal structure and surface topography of canine skin. *Research in Veterinary Science* 1982;33:99-104.

Loh ZHK, Allan GS, Nicoll RG *et al*. Ultrasonographic characteristics of soft tissue tumours in dogs. *Australian Vet J* 2009;87:323-329.

Mandava A, Konathan R, Neelala K. Utility of high-resolution ultrasonography and colour Doppler in the assessment of pigmented skin lesions. *Ultrasound* 2012;20:155-160.

Mandava A, Prabhakar RR, Konathan R. High-resolution ultrasound imaging of cutaneous lesions. *Indian J Radiol Imaging* 2013;23:269-277.

Marconato L, Rossi F, Bettini G, *et al*: Mastocitoma. In: Marconato L and Amadori D, editors. *Oncologia medica veterinaria e comparata*. 1st edn. Poletto editore, Milano, 2012:282-307(a). Marconato L, Rossi F, Bettini G, *et al*: Tumori della cute. In: Marconato L and Amadori D, editors. *Oncologia medica veterinaria e comparata*. 1st edn. Poletto editore, Milano, 2012:240-281(b).

Marconato L, Rossi F, Bettini G, *et al*: Tumori del sottocute. In: Marconato L and Amadori D, editors. *Oncologia medica veterinaria e comparata*. 1st edn. Poletto editore, Milano, 2012:308-328 (c).

Marconato L, Rossi F, Bettini G, *et al*: Disordini istiocitari. In: Marconato L and Amadori D, editors. *Oncologia medica veterinaria e comparata*. 1st edn. Poletto editore, Milano, 2012:874-890 (d).

Marconato: Sindromi paraneoplastiche. In: Marconato L and Amadori D, editors. *Oncologia medica veterinaria e comparata*. 1st edn. Poletto editore, Milano, 2012:104-127.

Martini MC. Anatomia i fizjologia skóry. In: Martini MC, editor. Kosmetologia i farmakologia skóry. Warszawa: Wydawnictwo Lekarskie PZWL 2007:37–59.

Mason I.S., Lloyd D.H. Scanning electron microscopical studies of the living epidermis and stratum corneum of dogs. In: Ihrke P.J., Mason I.S., White S.D. eds. *Advances in Veterinary Dermatology* 1993:131-139.

Matteucci ML, Spaulding K, Dassler C, *et al*. Ultrasound diagnosis: intra-abdominal wood foreign body. *Vet Radiol Ultrasound* 1999;40:513-516.

McTighe S, Chernev I. Intramuscular lipoma: A review of the literature. *Orthop Rev* 2014;6:156-163.

Medleau L, Hnilica KA. (eds) Dermatologia del cane e del gatto. 2nd edn. Elsevier-Masson, 2007.

Milner SM, Memar OM, Gherardini G, *et al*. The histological interpretation of high frequency cutaneous ultrasound imaging. *Dermatol Surg* 1997;23:43–45.

Miyauchi S, Tada M, Miki Y. Echographic evaluation of nodular lesions of the skin. *J Dermatol* 1983;10:221-227.

Mlosek RK, Malinowska S. Ultrasound image of the skin, apparatus and imaging basics. *J Ultrason* 2013;13:212–221.

Moe L, Lium B. Hereditary multifocal renal cystadenocarcinomas and nodular dermatofibrosis in 51 German Sheperd dogs. *J Small Anim Pract* 1997;38:498-505.

Mohammed SI, Meloni GB, Pinna Parpaglia ML, *et al*. Mammography and ultrasound imaging of preinvasive and invasive canine spontaneous mammary cancer and their similarities to human breast cancer. Cancer Prev Res 2011;4:1790-1798.

Namazi F, Hasiri MA, Oryan A, *et al*. Hemangiopericytoma in a young dog: Evaluation of histopathological and immunohistochemical features. *Vet Res Forum* 2014;5:157–160.

Nazarian LN, Alexander AA, Kurtz AB, *et al*. Superficial melanoma metastases: Appearances on Gray-scale and Coloro Doppler Sonography. *AJR* 1998;170:459-463.

Neuber A. Panniculitis in dogs and cats. *Companion Animal* 2011;16:27-30.

Nishiya AT, Massoco CO, Felizzola CR, *et al*.Comparative Aspects of Canine Melanoma. *Vet Sci* 2016;3,7;doi:10.3390/vetsci3010007.

Nowicki A. Wstęp do ultrasonografii. Podstawy fizyczne i instrumentacja. Warszawa: MediPage; 2004.

Nyman HT, Kristensen AT, Lee MH, *et al*. Characterization of canine superficial tumors using gray-scale b mode, color flow mapping, and spectral doppler ultrasonography—a multivariate study. *Vet Rad Ultrasound* 2006;47:192–198.

O'Kell AL, Inteeworn N, Diaz SF, *et al*. Canine sterile nodular panniculitis: a retrospective study of 14 cases. *J Vet Intern Med* 2010;24:278-284.

Ohlerth S, Kaser-Hotz B. A review of Doppler sonography for the assessment of tumour vascularity. *Vet Comp Oncol* 2003;1:121-130.

Paltiel HJ, Burrows, Kozakewich HP, *et al.* Soft-tissue vascular anomalies: utility of US for diagnosis. *Radiology* 2000;214:747-754.

Park JK, Hong IH, Ki MR, *et al*. Multiple perianal infundibular follicular cysts in a dog. *Vet Dermatology* 2010;21:303-306.

Paterson S. Skin diaseses of the dog. 1st edn. Wiley, Blackwell Science,1998.

Poziniak MA, Crass JR, Zagzebsky J, et al. Clinical efficacy of Kitecko ultrasonic conductor. *Invest Radiol* 1989;24:128–132.

Radu B, Maria C, Monica L, *et al*. Diagnosis and characterization of cutaneous tumors using combined ultrasonographic procedures (conventional and high resolution ultrasonography). *Med Ultrason.* 2010;12:317–22.

Rahul K, Panda A, Handa N, *et al*. Epidermal inclusion cyst in a male breast: parallel linear echoes (tram-track appearance) on sonography as a diagnostic clue. *BMJ Case Rep* 2015; doi:10.1136/bcr-2015-213045.

Raskin RE. Skin and subcutaneous tissue. In: Raskin R, Meyer DJ, eds. *Canine and feline cytology: A colour atlas and interpretation guide.* 3rd edition. Elsevier Saunders, 2016;34-90.

Reed LT, Knapp DW, Miller MA. Cutaneous Metastasis of Transitional Cell Carcinoma in 12 Dogs. *Veterinary Pathology* 2012;50:676-681.

Rogers KS. Mast cell disease. In: Ettinger SJ, Fieldman EC, eds. *Textbook of veterinary internal medicine*. 7th edn. Elsevier Saunders, 2010;2193-2199.

Rook A, Wilkinson DS, Ebling FJG. Textbook of Dermatology. Oxford, England: Blackwell; 1968.

Schmid-Wendtner MH and Burgdorf W. Ultrasound scanning in dermatology. *Arch Dermatol* 2005;141:217-224.

Scott DW, Miller WH, Griffin CE. Structure and function of the skin. In: Scott DW, Miller WH, Griffin CE, eds. *Muller and Kirk's small animal dermatology*. 6th edn. Philadelphia: WB Saunders Co, 2001:1–70.

Seidenari S, Pagnoni A, Di Nardo A, *et al*. Echographic evaluation with image analysis of the normal skin: variation according to age and sex. *Skin Pharmacol* 1994;7:201–209.

Shah ZR, Crass JR, Oravec DC, *et al*. Ultrasonographic detection of foreign bodies in soft tissue using turkey muscle as a model. *Vet Radiol Ultrasound* 1992;33:94-100.

Shiels WE, Babcock DS, Wilson JL, *et al*. Localization and guided removal of soft-tissue foreign bodies with sonography. *Am J Roentgenol* 1990;155:1277-1281.

Simko E, Wilcock BP, Yager, JA. A retrospective study of 44 canine apocrine sweat gland adenocarcinomas. *Can Vet J* 2003;44:38–42.

Stiller MJ, Gropper CA, Shupack JL, Lizzi F, Driller J, Rorke M. Diagnostic ultrasound in dermatology: Current uses and future potential. *Cutis* 1994;53:44-48.

Summers JF, Brodbelt DC, Forsythe PJ, Loeffler A, Hendricks A. The effectiveness of systemic antimicrobial treatment in canine superficial and deep pyoderma: a systematic review. *Vet Dermatol* 2012;23:305-329.

Surov A, Kohler J, Wienke A, *et al*. Muscle metastases: comparison of features in different primary tumours. *Cancer Imaging* 2014;14:21.

Szymañska E, Nowicki A, Mlosek K, *et al*. Skin imaging with high-frequency ultrasound-Preliminary results. *Eur J Ultrasound* 2000;12:9-16.

Tavasoly A, Gholami H, Rostami Amir, *et al*. Clinico-histopathologic and outcome features of cutaneous infundibular keratinizing acanthoma: a case report and literature review *World J Surg Oncol* 2014;12:173.

Thomson MJ, Withrow SJ, Dernell WS, Powers BE. Intermuscular lipomas of the thigh region in dogs: 11 cases. *J Am Anim Hosp Assoc* 1999;35:165–167.

Tunio MA, Asiri MA, Riaz K, *et al*. Skeletal muscle metastasis secondary to adenocarcinoma of colon: a case report and review of literature. *J Gastroint Dig Syst* 2013;S12:002.

Turek MM. Cutaneous paraneoplastic syndromes in dogs and cats: a review of the literature. *Vet Dermatol* 2003;14:279-296.

Vignoli M, Terragni R, Rossi F, *et al*. Whole body computed tomographic characteristics of skeletal and cardiac muscular metastatic neoplasia in dogs and cats. *Vet Radiol Ultrasound* 2013;54:223-230.

Volta A, Bonazzi M, Gnudi G, *et al*. Ultrasonographic features of canine lipomas. *Vet Radiol Ultrasound* 2006;47:589-591.

Weiss SW. Lipomatous tumors. *Monogr Pathol* 1996;38:207–239.

Welle M, Bley CR, Howard J, *et al*. Canine mast cell tumours: a review of the pathogenesis, clinical features, pathology and treatment. *Vet Dermatol* 2008;19:321-339.

Wortsman X. Sonography of cutaneous and ungual lumps and Bumps. *Ultrasound Clin* 2012;7:505-523.

Wortsman X and Wortsman J. Skin imaging. Inn: Dogra VS, Gaitini D, eds. Musculoskeletal Ultrasound with MRI correlation. 1st edn. New York: Thieme 2010:147-170.

Wortsman X, Wortsman J, Matsuoka L, *et al*. Sonography in pathologies of scalp and hair. *Br J Radiol* 2012;85:647-655.

Wortsman X and Bouer M. Common benign non-vascular skin tumors. In: Wortsman X and Jemec G. *Dermatologic Ultrasound with Clinical and Histologic Correlations*. Ed. Springer, New York, 2013:119-175.

Yardimci C, Yardimci C, Aksoy O. Clinical and pathological evaluation of the injection site masses in 12 dogs. *Revué de Médicine Vétérinaire* 2011;162:508-513.

Young, LA, Dodge J, Guest K, *et al*. Age, breed, sex and period effects on skin biophysical parameters for dogs fed canned dog food. *J Nutr* 2002;132:1695S-1697S.

Yuan WH, Hsu HC, Lai YC *et al*. Differences in sonographic features of ruptured and unruptured epidermal cyst. *J Ultrasound Med* 2012;31:265-272.

Zwingerberger A, Benigni L, Lamb CR. Musculoskeletal system. In Matoon JS and Nyland TG (eds). *Small Animal Diagnostic Ultrasound*. 3rd edn. Elsevier, 2015:517-540.

# SITOGRAPHY

sonoskin.com. **Skin Ultrasound, The dermatologic ultrasound website**. Last visit 5th December 2016, website: http://www.sonoskin.com

# ACKNOWLEDGEMENTS

I would like to express my special appreciation and thanks to my advisor Prof. Antonella Volta, you have been a tremendous mentor for me. I would like to thank you for encouraging my research and for allowing me to grow as a research scientist.

I would especially like to thank physicians of the Veterinary Teaching Hospital of Parma. All of you have been there to support me when I recruited patients and collected data for my Ph.D. thesis.

A special thanks to my family. Words cannot express how grateful I am to my mom, dad, my brother and my grandparents for providing me with unfailing support and continuous encouragement throughout my years of study and through the process of researching and writing this thesis. This accomplishment would not have been possible without them.

Finally, I would also like to thank all of my friends who supported me in writing, and incented me to strive towards my goal.